Volume 23 Issue 37
Originally issued as B5



Global Journal of human-social science: b
Geography, Geo-Sciences, Environmental Science & Disaster Management
Volume 23 Issue 5 Version 1.0 Year 2023
Type: Double Blind Peer Reviewed International Research Journal
Publisher: Global Journals
Online ISSN: 2249-460x & Print ISSN: 0975-587X

Morphotectonic Processes in Seismic Zones of ModerateIntensity, Argentina

By Adolfo Antonio Gutiérrez
Universidad Nacional de Tucumán

Abstract- This study deals with the neotectonic deformation in seismic zones of moderate intensity in some areas of the Sierras Pampeanas, Santa Bárbara System and Chaqueña Plain of Argentina. In the study region, the location of earthquakes of ≥ three, ≥ four, and ≥ six Richter magnitudes agree with the traces of regional faults, evidencing their neotectonic activity. Seismic energy is generally transmitted over inherited faults, such as in the Metan basin. Minor new faults occur in Quaternary terraced deposits, and others move, taking advantage of the Neogene sedimentary strata. The folds are generally buried, but the younger sequences are gently undulating. The seismic energy dissipated through fewer cohesion materials that form the valleys' fill, developing discrete fault scarps and strongly folded conglomerate strata. The foothills deposits and basins absorbed most of the seismic energy released during the reactivation of the faults. Tectonic activity is deforming 630 BP deposits in the Cumbres Calchaquíes piedmont.

Keywords: *neotectonics. earthquakes. andean foreland. natural hazards.*

GJHSS-B Classification: *LCC: QE521-545*



Strictly as per the compliance and regulations of:



© 2023. Adolfo Antonio Gutiérrez. This research/review article is distributed under the terms of the Attribution-NonCommercial-NoDerivatives 4.0 International (CC BY-NC-ND 4.0). You must give appropriate credit to authors and reference this article if parts of the article are reproduced in any manner. Applicable licensing terms are at https://creativecommons.org/licenses/by-nc-nd/4.0/.

Morphotectonic Processes in Seismic Zones of Moderate Intensity, Argentina

Adolfo Antonio Gutiérrez

Abstract- This study deals with the neotectonic deformation in seismic zones of moderate intensity in some areas of the Sierras Pampeanas, Santa Bárbara System and Chaqueña Plain of Argentina. In the study region, the location of earthquakes of≥ three, ≥ four, and ≥ six Richter magnitudes agree with the traces of regional faults, evidencing their neotectonic activity. Seismic energy is generally transmitted over inherited faults, such as in the Metan basin. Minor new faults occur in Quaternary terraced deposits, and others move, taking advantage of the Neogene sedimentary strata. The folds are generally buried, but the younger sequences are gently undulating. The seismic energy dissipated through fewer cohesion materials that form the valleys' fill, developing discrete fault scarps and strongly folded conglomerate strata. The foothills deposits and basins absorbed most of the seismic energy released during the reactivation of the faults. Tectonic activity is deforming 630 BP deposits in the Cumbres Calchaquíes piedmont. Considering deformation values, neotectonic deformation in the outcrops and seismic profiles evidence, it is possible to interpret that the seismic activity in the study area from the Pleistocene to the present remained between the current records. This seismic activity, sustained over time, is sufficient to produce deformation in the foothills, reactivate pre-existing faults with small displacements and generate minor new faults in recent conglomeratic deposits. Many faults are blind. However, the deformation of the landscape and the modification of the drainage network are direct indicators of the activity of these structures.

Keywords: neotectonics. earthquakes. andean foreland. natural hazards.

I. Introduction

The deformation of the Andean foreland by neotectonics processes has been treated extensively in the literature. This evidence the interest of the scientific community in understanding tectonic rotations, the direction of tectonic shortening, depths of the detachment of the main structures, the position of the front deformation, vergence of the structures, seismic activity associated with the movements of the faults and deformations of the mountain fronts.

In the plate tectonics context, subjected to compressive stress with NE strike during the Cenozoic, the study area coincides with the latitude where the Nazca plates change the angle dip, high angle north of 27° S and the low angle at south (Schwanghart and Scherler, 2014; Somoza and Ghidella, 2005) (Figure 1). Strecker et al. (1989) and Mon (1993) agree that the faults that raise the edges of the mountain ranges could be reactivated Palaeozoic structures. Marrett et al. (1994) document for northwestern Argentina two kinematic regimes that characterise the late Cenozoic deformation, a WNW shortening and a strike-slip phase with ENE shortening. The tectonic deformation that was active since the Middle Eocene (Del Papa et al., 2005) was migrating from the Puna towards the east (Carrapa et al., 2005; Deeken et al., 2006; Carrapa and De Celles, 2015), modifying, in the Miocene, the drainage network of the western edge of the Eastern Cordillera (Jordan and Alonso, 1987; Starck and Vergani, 1996; Carrera and Muñoz, 2008; Carrapa et al., 2011; Pearson et al., 2013).

An approximation of the evolution of neotectonic deformation in the Eastern Cordillera is obtained by recording GPS (Global Positioning System) speeds that decrease from 10 to 4 mm/yr (McFarland and Bennett, 2017). Other authors also estimated the rates of shortening in the region. Echavarria et al. (2003) obtained shortening rates for the Quaternary of the Sub-Andean System of Argentina between 8 and 11 mm/yr. Pearson et al. (2013) calculated the shortening rates at latitude 25-26° S and obtained averages of 6.5 mm/y from 12 to 4 Ma and 3.6 mm/y from 4 Ma to the Holocene. Uplift rates for the Late Pleistocene–Holocene were determined by (García et al., 2013; García et al., 2019) obtaining values of 0.3 to 0.7 mm/yr in the Lerma Valley. In the Lomas de Olmedo, shortening rates of 2.34 mm/yr for most of the Holocene was calculated (Ramos et al., 2006). According to the seismic classification for Argentina, based on studies carried out until 1983, except for the areas surrounding the cities of Salta and San Salvador de Jujuy, the north and a large part of the Sierras Pampeanas are in Zone 2 of moderate danger and Chaqueña Plain in Zone 1 reduced risk (INPRES, 2018).

Author: Facultad de Ciencias Naturales e IML, Universidad Nacional de Tucumán, Miguel Lillo 205,4000 San Miguel de Tucumán, Argentina.
e-mail: gutierrez.aa@hotmail.com

© 2023 Global Journals

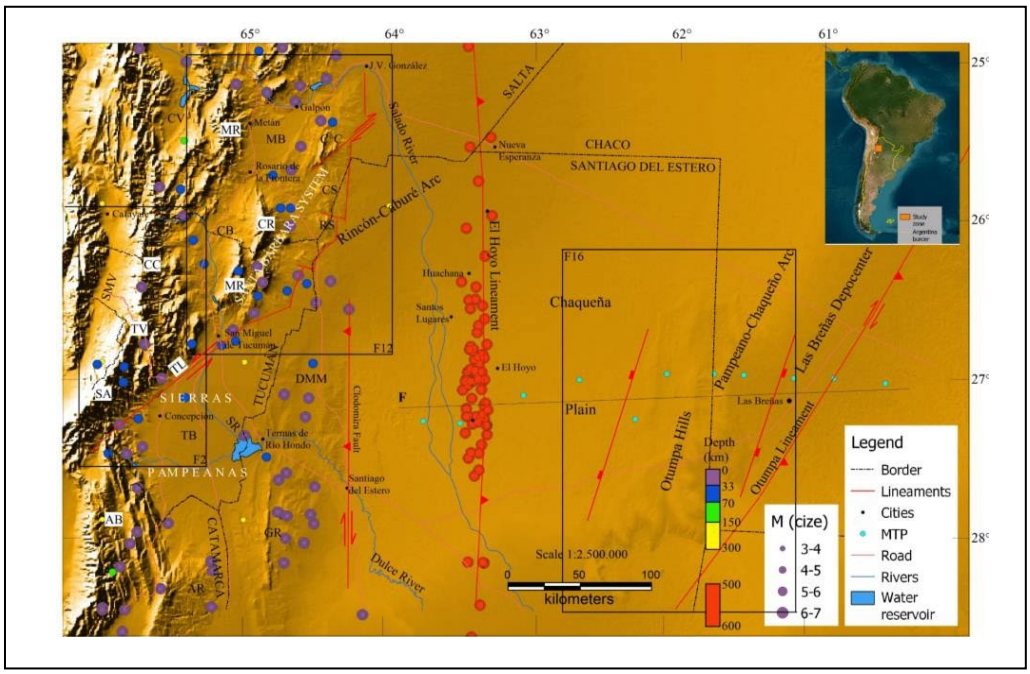


Figure 1: Regional location of the study area. The morphotectonic map shows the significant orographic units and the regional structures that mark the contact between the Andean front and the Chacopampeana Plain. MTP: Magnetotelluric profile. With coloured circles, the epicentres ofthe earthquakes are located. The depth of the earthquakes is indicated with a colour scale, and their magnitudes with grey circles. A box with black lines indicates the location of the figures (F12). CV: Calchaquí Valley. MR: Metán Range. MB: Metán Basin. C°C: Cerro Colorado. CC: Cumbres Calchaquíes. CB: Choromoro Basin. CR: La Candelaria Range. MR: Medina Range. SMV: Santa María Valley. TV: Tafi Valley. SA: Sierra de Aconquija. TL: Tucumán Lineament. SR: SalíRiver. DMM: Dorsal Mujer Muerta. TB: Tucumán Basin. AB: Ambato Block. AR: Ancasti Range. F: Profile, Figure 19.

In the seismogenic region of the continental crust (15–18 km), earthquakes produce an episodic rigid frictional deformation (Sibson, 1982; Scholz, 2002) whose rupture by propagation during deformation is controlled by the anisotropic fabric at the cortical scale (Allen and Shaw, 2011). When an earthquake is generated, oscillations occur in existing faults or, less frequently, in new faults (Scholz, 2002; Brace and Byerlee, 1966), the elastic stress accumulating in the rocks surrounding the fault zone until the resulting stress in the plane exceeds its frictional resistance and failure occurs (Fagereng and Toy, 2011).

The conditions of the shear stress (rf) at which the failure is going to slip are indicated bythe equation (Eq. (1)):

$$rf = C^{\circ} + \mu_S(\sigma n - Pf), \quad (1)$$

Where C° is the cohesion force, μ_S is the coefficient of static friction, σn is normal effort, and Pf is the fluid pressure (Fagereng and Toy, 2011), high fluid pressures would favour the reactivation of faults, reducing the cohesion force (Nortje et al., 2011). However, for new faults to form in a region where faults already exist, it is required that those old faults develop sufficient cohesion and have insufficient fluid pressure in the pores in such a way as to prevent them from reactivating, even with favourable orientations (Nortje et al., 2011). It was also suggested that themigration of the fault activity towards the foothills is due to the cessation of movement of the faults of the mountain fronts, with these new structures inheriting the style of the primary faults (Costa, 2019). Most earthquakes result from increased shear displacement in the fault (Ambraseys and Tchalenko, 1969), generating rupture and slip that are roughly related to the magnitude of the earthquake (Wells and Coppersmith, 1994; Hanks and Kanamori, 1979) (Table 1).

Zeckra (2020) installed a temporary seismic network in the Santa Bárbara System and discovered high seismic activity confined along the Andean thrust front. The catalogue of locations of primary hypocenters, with a magnitude of completion MC 1.45, allowed him to interpret the distribution of events along steep and deep thrust faults generated through the inversion of Cretaceous normal faults.

Table 1: Approximate source parameters for different magnitude earthquakes (partial magnitudes), with average stress drop (3 MPa) over a circular rupture [Length (L) = Width (W)] (Fagereng and Toy, 2011; Wells and Coppersmith, 1994).

Magnitude of Mw	Average slip (cm)	L=W
5	10	3 km
4	3	1 km
3	1	30 m

© 2023 Global Journals

Our work shows the differential deformation in the mountain front due to the propagation of seismic energy through basins, foothills deposits, and fault reactivations. The cohesion of the geological material is considered relevant for the propagation of the seismic energy produced by the activity of the faults. The moderate seismic energy transmitted by the faults, but sustained over time, is sufficient to make morphostructural changes in the landscape. This moderate energy is transferred and generates changes in less cohesive materials. This moderate energy was maintained with magnitudes similar to those in the study region, probably since the Pleistocene. We take as examples the neotectonic activity in the north of Sierras Pampeanas (Tafí and Amaicha valleys and the structural relationship between the Cumbres Calchaquíes and Sierra de Aconquija), Santa Bárbara System (Cerro Colorado, Metán basin, La Candelaria Range, and Choromoro basin), and the Chaqueña Plain (Otumpa Hills) (Figure 1).

Different effects of seismic wave propagation are observed in the study area. We shownew structures with vertical and horizontal components and fold morphologies generated in allthese areas. They occur in basins and the foothills, close to regional structures on the mountain front. Other recent and recurrent evidence of tectonic activity in the region is river captures (Gutiérrez et al., 2003), landslides, and retrograde erosion. We observe that earthquakes are aligned with regional structures.

II. Methodology

The research was carried out based on the collection of bibliographic antecedents, interpretation of satellite images, and field data surveys. To develop thematic cartography, the visual and digital interpretation of satellite images LANDSAT 8, SENTINEL 1, and RADARSAT was carried out. The digital treatment for the visual interpretation of the LANDSAT and SENTINEL images consisted of combining different bands. All satellite and radar images were interpreted using the QGis software; then, thematic maps were drawn. To prepare the topographic profiles, we used high-resolution digital elevation models (12.5 m) provided by the ALOS PALSAR mission. During fieldwork, the surfaces deformed by neotectonic processes were identified (fault steps, landslide zones, deformed foothills, whale-back morphologies in alluvial fans, erosion of conglomerate terraces, and transport of rolling by surface drainage, development of drainage networks as indicators of deformation) and data on the structures that generated these morphologies were collected. We collect information on the seismicity around the study area, recording only earthquakes with magnitudes between 2 and 7 (IRIS, 2020) (Figure 1). Four earthquakes of magnitude ≥ six were recorded at 0 to 33 km depths. And eight at 500 to 600 km (Table 2) (Figure 1). Between 300 and 500 km deep, a zone of seismic silence is observed (Table 2).

Table 2: Seismic frequency of occurrence.

Depth (km)	Total	Magnitude of Mw
0-33	68	3.3 - 6.12
33-70	33	4.0 - 5.9
70-150	2	4.3
150-300	4	2.2 - 3.0
300-500	Silence	---
500-600	76	3.8 - 6.9

III. Regional Tectonic Mophology

In the north of the Sierras Pampeanas, the Sierra de Aconquija and Cumbres Calchaquíesseem to have formed a single mountain block with an NNE strike and slightly curved, concave towards the west. It has been raised by high-angle, double-vergent, reverse faults on both edges (Lavenu, 2006; Cristallini et al., 2004), Cumbres Calchaquíes and Aconquija faults on the western border and Periquillo fault on the eastern boundary (Figure 2).

Probably in the Pleistocene, the drainage system developed on the eastern edge of the Cumbres Calchaquíes, Sierra de Aconquija, and Ambato block had an approximate general direction towards the east and ended in the Chaco plain, covering a large area of surface runoff, maintaining the contribution of coarse sediments by the continuous uplift of the mountain systemand appropriate climatic conditions (Gutiérrez et al., 2003). The records of these hydrogeological processes are the thick conglomerate deposits arranged in the upper parts of the Los Sosa River terraces, eroded by the current surface runoff. Later, with the progress of tectonic activity, this drainage system completely eroded, configuring the current network (Gutiérrez et al., 2003).

In the Santa Bárbara System, the mountainous belt shows two sections: the northern one with thick Cretaceous sequences and the southern one with no Cretaceous layers, and the Tertiary lies directly on Paleozoic rocks (Figure 1). The evolution of this part of the Santa Bárbara System began in the middle Eocene, coinciding with a tectonic pillar that was already elevated at this time. The Andean shortening in the last 5 Ma caused a NE strike fault generating dextral displacements that, in turn, originated complex structures. To the west, the Metán Basin and the Choromoro Valley separate it from the Eastern Cordillera and Sierras Pampeanas. To the east, the Chaco Plain extends (Mon and Gutiérrez, 2007).

© 2023 Global Journals

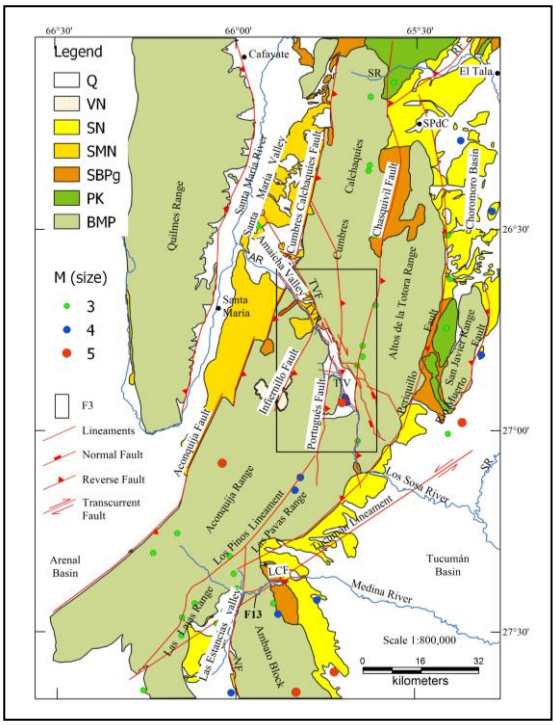


Figure 2: Morphotectonic map of the Sierra de Aconquija and Cumbres Calchaquíes. It shows the depressions of Tafí and Amaicha and the regional structures that gave rise to them. In addition, they do indicate the larger geological units that condition the fracturing that gave rise to the valleys. The location of seismic epicentres and their magnitudes are shown. Q: Fluvio-eolian deposits, Quaternary. VN: volcanic rocks, Neogene. SN: Sedimentary, Neogene. SMN: Santa María Group, Neogene. SBP: Santa Bárbara Subgroup, Paleogene. PK: Pirgua Subgroup, Cretaceous. BMP: Metamorphic Basement, Proterozoic. 3, 4, and 5M: Seismic magnitude. SR: Salí River. SPdC: San Pedro de Colalao. RF: Rearte Fault. AR: Amaicha River. TVF: Tafí del Valle Fault. TVR: Tafí del Valle River. TV: Tafí Valley. LCF: Las Cañas Fault. F3: Figure 3 location. F13: Figure 13 location.

The Chaqueña Plain's sedimentary basin constitutes the Andean front's foothills. The topographic relief rises just 200 m a.s.l. in the Otumpa Hills (Figure 1). Towards the southeast, the Pampean-Chaqueño Arc stands out, which rises above the Las Breñas Basin with the Otumpa Lineament (Figure 1) (Pezzi and Mozetic, 1989; Chebli et al., 1999). With the magnetotelluric data obtained, Pomposiello et al. (2010) interpret that the marked lateral discontinuity observed in the resistivity model could represent the boundary between the Río de la Plata craton and the Pampean terrane or another Precambrian cratonic fragment (Figure 1). In the central western zone of the Chaqueña Plain, there is an N-S strip of seismic epicentres of more than 500 km in length, originating between 500 and 600 km in depth (Figure 1). It is the highest seismic frequency in the study area and where the most intense earthquakes occur (Table 2). Peri (2012) hypothesises that these earthquakes are linked to the presence of the Pacific slab at depth (Figure 1). Based on the marked N-S linearity of these seismic epicentres and the coincidence with one of the high resistivity zones of the 2D magnetotelluric model (Pomposiello et al., 2010), the existence of a blind structure El Hoyo Lineament was interpreted (Figure 1).

IV. Quaternary Deformations

Numerous works document the recent tectonic activity in the Geological Provinces of Argentina that occur in the foothills, in the intra and intermontane basins, or also refer to the geological processes triggered on the mountain fronts by active seismic activity, such as landslides in the slopes of the mountains, formation of dikes by obstruction of rivers, etc. The earthquake rupture zone is not located in the central fault zone of the mountain front but on theflank of the mountain range (Kamb et al., 1971), in a new fault zone called FAF (frontal active fault/flexure) that is generated due to the marked difference in stiffness between the piedmont and basement deposits (Costa, 2019; Ikeda, 1983).

On the southeastern edge of the Precordillera, the Neogene strata ride on quaternary deposits of the foothills of the mountain front and, in the Sierra Chica de Córdoba, Sierras Pampeanas, the most recent deformations linked to the Sierra Chica fault system is not located in the topographic break of the mountain slope, but usually appear associated with a secondary structure (Costa, 2000; Costa et al., 2014; Costa, 2019;). The topographic growth in the sedimentary basins on the eastern edge of the Sierras Pampeanas shows the progressive deformation towards the east, obstructing and diverting surface drainage. The Alto de Mansilla isa topographic elevation just 130 m high. It was generated by convergent heading faults and overlapped with step-over restraining bend geometry, dividing a large lake into the Salinas Grandes and Salinas de Ambargasta (Gutiérrez et al., 2017). In the south end of the Sierra de Aconquija, thick conglomeratic piedmont deposits were deposited during the Pliocene-Pleistocene and were deformed and detached from their contribution areas by neotectonics (Gutiérrez et al., 2023).

In the Tafí and Amaicha valleys (Figures 2 and 3), in the foothills of the south end of the Cumbres Calchaquíes, the surface relief is disturbed by structures that were generated during neotectonic activity that give the landscape a morphology that breaks the monotony of the forms caused by alluvial fans and the fluvio-aeolian erosion (Gutiérrez et al., 2021). In the alluvial fans of the foothills of the La Candelaria range (Santa Bárbara System), topographic highlights attributed to neotectonic activity and related to seismic events were observed (Gutiérrez et al., 1997).

The sedimentary cover in the Cretaceous Rift basins is very thick (3554 m in the Metán basin, 3000 m

© 2023 Global Journals

in the Choromoro basin, and 7000 m in the Tucumán basin) (Iaffa et al., 2011; Iaffa et al., 2011; Abascal, 2005), so the Neogene and Quaternary deformation folded these sedimentary piles, laying them on the Proterozoic-Paleozoic basement that is exposed in small outcrops, in the upper parts of the mountains. This tectonic morphology is mainly due to the inverse reactivation of normal faults inherited from the Cretaceous Rift, sometimes blind (Iaffa et al., 2011; Abascal, 2005; Grier et al., 1991). In the Metán basin, recent deformation was documented in folded surfaces, associated with blind and inherited structures. A case study with deep seismic and shallow geophysical prospecting methods evidenced the deformation produced by the El Galpón fault, folding neogenic and quaternary units, which would have experienced a seismic movement of M 5.7 in 2015 (Zeckra, 2020).

In the Cafayate valley, the Quaternary deformation produced folds in the lake deposits from the Upper Pleistocene to the Middle Holocene, evidencing the reactivation of the main high-angle faults, verging to the west, of the eastern edge of the valley, generating secondary faults that affect the quaternary coverage (Figueroa-Villegas et al., 2017).

Sierras Pampeanas (Cumbres Calchaquíes – Sierra de Aconquija)

a) Regional Geology

The Cumbres Calchaquíes, Sierra de Aconquija, and Ambato Block ranges are made up of an igneous-metamorphic basement (Upper Proterozoic-Lower Paleozoic) (Mon and Drozdzewski, 1999; Turner, 1960) (Figure 2). Sediments from the Cretaceous Rift could not have covered these mountain ranges because they were elevated (Gutiérrez et al., 2019; Mon et al., 2012), the outcrops of the Pirgua Subgroup of the Salta Group reached the northern end of the Cumbres Calchaquíes and the western edge of the Sierra de San Javier (Figure 2).

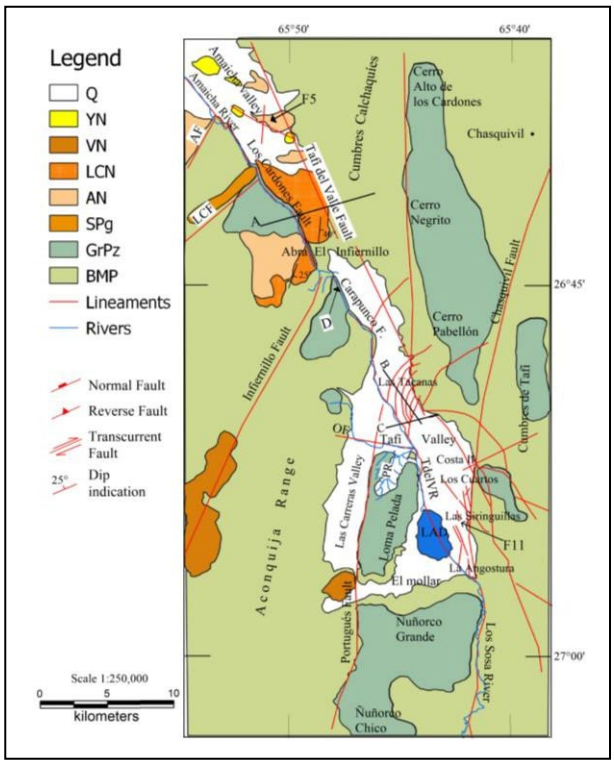


Figure 3: Morphotectonic map of the Tafí and Amaicha valleys. It shows the depressions of Tafíand Amaicha and the regional structures that gave rise to them. In addition, they do indicate the larger geological units that condition the fracturing that gave rise to the valleys. In this scheme, the recently generated structures deforming the foothills were drawn with red lines. Q: Fluvio- eolian deposits, Quaternary. YN: Yasyamayo Formation, Neogene. VN: Volcanic rocks, Neogene. LCN: Los Corrales Formation, Neogene. AN: Andalhuala Formation, Neogene. SPg: Saladillo Formation, Paleogene. GrPz: Paleozoic granites. BMP: Proterozoic early – Paleozoic Basement. AF: Aconquija Fault. LCF: Los Corpitos Fault. LAD: La Angostura Dam. OF: Ovejería Fault. PR: Pelado River. A: Profile Figure 4. B: Profile Figure 6. C: Profile Figure 8. D: Profile Figure F10. F5: Profile Figure 5 location. F11: Figure 11 location.

Neogene sediments occupied the Choromoro and Las Estancias basins in Tucumán and the Santa María basin in Catamarca (Gutiérrez et al., 2019). In the Santa María valley, the sedimentary sequence overlaps the metamorphic basement towards the Amaicha valley, reachingthe Infiernillo pass (Mon et al., 2012; Aceñolaza and Toselli, 1981; Porto et al., 1982), while in the northern end from the Sierra de Aconquija, the volcanism that gave rise to the extrusive rocks of Cerro Las Ánimas occurred ca. 13 Ma (Gutiérrez et al., 2019; González, 1990). The sedimentary column of the Santa María Valley was ordered in Sequences by Bossi et al. (2001) (Table 3).

The Tafí and Amaicha Valleys are intramontane tectonic basins at the Sierras Pampeanas' northern end (Figures 1, 2). The Tafí Valley is independent of the Amaicha Valley; the water sub-basins of both valleys

© 2023 Global Journals

have springs in the Infiernillo pass (Figure 2). The waters of the Amaicha Valley are part of the Plata basin through the Santa María, Las Conchas, and Salado rivers, and the waters of the Tafí Valley ending in the Salí - Dulce River, forming part of the endorheic basin of the Mar Chiquita lagoon (Gutiérrez et al., 2017; Bossi et al., 2001).

b) Regional structures

Currently, the Sierra de Aconquija-Cumbres Calchaquíes mountain range is separated at the western edge, where it opens towards the Santa María Valley through the Amaicha Valley (Figure 2). On the eastern border, it remains together, but both mountains are unlinked by the Tafí del Valle fault (Figure 2). The north end of the Ambato Block joins the southeastern edge of the Sierra de Aconquija through the Tucuman Lineament (Figure 2).

Two faults limit the Sierra de Aconquija and Cumbres Calchaquíes mountains; the Tafídel Valle fault marks the southern edge of the Cumbres Calchaquíes, and the Los Cardones (Amaicha valley) and Carapunco (Tafí valley) faults the north edge of the Sierra de Aconquija(Gutiérrez et al., 2021) (Figure 3).

The Tafí del Valle fault zone has evidence of variations along strike, proved by the interpretation of satellite images, surface geometry, and the rock outcrops in the Tafí and Amaicha valleys. A single plane separates the Sierra de Aconquija from the Cumbres Calchaquíes in the southeastern end. It was possible to measure the fault plane in a stream at theentrance to the Tafí valley, registering the following values (225°/88°, 228°/85°) (Figures 2, 3) (Gutiérrez et al., 2021).

In the north end of the Tafí valley, at the foot of the fault, a vast deposit of piedmont develops, reaching 23 km in length and extending between 2 and 4 km in width. These depositsare assumed to be arranged on a metamorphic basement hiding the fault plane (Figure 3). In theAmaicha Valley, the fault zone is about 6 km wide, hosts the upper sequence of the Santa María Group, and opens towards the Santa María Valley, where the dextral transcurrent geometry of the fault was verified (Mon et al., 2012) (Figure 3).

Table 3: Stratigraphic sequence of the Santa María Group according to Bossi et al. (Bossi et al., 2001). Datings made by Powell and González (1997), Spagnuolo et al. (2015), Georgieff and Díaz (2014), Butler et al. (1984), Marshall and Patterson (1981), Strecker et al. (1984). Identifying quaternary morpho-sedimentary units by Peña-Monné and Sampietro-Vattuone (2018) and Sampietro-Vattuone et al. (2019). Q: Quaternary.

ERA	Period/Epoch		Ma	Stratigraphy		
CENOZOIC	Q	Holocene	0.00006 0.0004 0.0013	H2 H1		
		Pleistocene	1.15	Tafí del Valle Formation Lomitas Pegadas Formation		
	NEOGENE	Pliocene	2.5 3.4	SANTA MARÍA GROUP	Sequence IV	Yasyamayo
			4.0		Sequence III	Los Corrales Upper Andalhuala
		Miocene	6.02 6.7 6.88 9.1		Sequence II	Lower Andalhuala Chiquimil Las Arcas San José
						Paranense
	PALEOGENE	Oligocene				
		Eocene			Sequence I	Saladillo Formation
		Paleocene	16	SANTA BÁRBARA GROUP		
Paleozoic - Proterozoic early				Basement		

Internally, the mountainous ensemble is also cut by regional NNE structures (Infiernillo, Portugués, Chasquivil faults, and Los Pinos lineament), which do not manage to separate them, but give the ensemble a morphology that allows identifying minor mountain ranges such as Las Lajas, Las Pavas and Altos de la Totora, which, had the initial deformation continued, would have formed independent units, as is the case with the San Javier range (Figure 2). In some cases, these structures gave rise to important rivers such as the Amaicha, Tafí del Valle-Los Sosa and Las Cañas rivers and, other times, they separate mountain blocks, such as the Los Pinos lineament that separates the Las Lajas and Santa Ana mountains from the Sierra de Aconquija (Figure 2).

The central zone of the Cumbres Calchaquíes and the northern end of the Sierra de Aconquija, crossed by the NNE structures, the Portuguese fault (to the west), and the Chasquivil fault (to the east), are intruded by granite bodies that constitute a strip with the same orientation as structures that limit them, where the Alto de los Cóndores, Negro, Pabellón, Loma Pelada, Ñuñorco Grande, and Ñuñorco Chico hills stand out (Figure 3).

A cortical extension was postulated in the early Miocene to explain the origin of Cenozoic basins in the northwestern Sierras Pampeanas that were inverted at approximately 5 Ma (Bossi et al., 2001; Ruiz-Huidobro, 1972; Gutiérrez and Mon, 2004). However, it is likely that these regional structures were partially active during the Cretaceous Rift but did not evolve sufficiently to form

© 2023 Global Journals

depocenters. For example, the Sierra de Aconquija and Cumbres Calchaquíes remained elevated during the Cretaceous because no outcrops of this age were found in the inner valleys (Mon et al., 2012). But, in all these regional NNE structures, spaces were generated during the Cretaceous Rift where small outcrops of red sandstones and conglomerate siltstones are preserved, attributed to the Santa Bárbara Subgroup of the Salta Group (Paleogene) (Figure 2). We can see them along the Aconquija and Cumbres Calchaquíes faults, in the Los Corpitos fault, on the eastern edge of the Los Pinos lineament and the east slope of the Santa Ana mountain range, on the northeastern border and southern end of the Chasquivil fault, in the Los Sosa riverbed and on the eastern edge of the Periquillo fault (Figures 2, 3). These reduced outcrops of red strata are attributed to the Santa Bárbara Subgroup and arranged on a metamorphic basement document. The other lower sequences of the Salta Group are not found in these regional structures. Possibly, in the Cretaceous Rift stage, the Aconquija, Cumbres Calchaquíes, Los Corpitos, Infiernillo, and Portugués faults constituted incipient steps that dipped towards the west, just as the Chasquivil fault represented a step dipping to the east, and the mountainous group remained elevated (Figures 2, 3). The granite bodies represented by the Alto de los Cardones, Negrito, Pabellón, Loma Pelada, Ñuñorco Grande, and Ñuñorco Chico hills constituted a longitudinal block towards which the steps of the normal faults converged, those that inclined to the east and those that sloped to the west (Figure 3). In the lower Tertiary, these small steps began to fill up with the sediments of the Santa Bárbara Subgroup. They were protected in the elevated parts of the slopes of the mountains, such as on the western edge of theSierra de Aconquija and Cumbres Calchaquíes, in the Los Corpitos fault. (Mon et al., 2012; Gutiérrez et al., 2019), in the Chasquivil fault and many other places (Figures 2, 3). Against the Infiernillo fault, the Santa María Group's upper sequence ends and fills the Amaicha Valley without reaching the Tafí Valley (Mon et al., 2012).

These areas of regional weakness, Cretaceous or Paleozoic, were reactivated with the Andean tectonics. Sometimes the normal faults of the Cretaceous Rift were reactivated in the same direction as the initial fault plane. Still, in the opposite sense (Iaffa et al., 2011; Abascal, 2005; Grier et al., 1991), and later on, these faults were cut by others with opposite sense and direction, such as the Aconquija, Cumbres Calchaquíes, and Infiernillo faults (Mon et al., 2012; Gutiérrez et al., 2019; Gutiérrez and Mon, 2004; Gutiérrez and Mon, 2008). However, the Chasquivil fault would have had a reverse reactivation because it arranged the preserved red strata in the Los Sosa River dipping 40° to the SE (Figure 3). Pilger (1984) interpreted that the uplift of the marginal mountain ranges to the Calchaquí Valley would have started at 13 Ma. The tectonic activity would have accelerated around 4 Ma, affecting the Yasyamayo Formation (ca. 1.5 Ma), therefore, would have occurred at approximately 1.2 Ma, extending to at least 0.6 Ma (Strecker et al., 1987) and the eastern edge of the Sierra de Aconquija began to rise at 9 Ma (Löbens et al., 2013) (Figure 3).

c) Amaicha valley

The Amaicha Valley, with an NW strike, extends to the northwest of the Tafí Valley, from the Infiernillo pass to the Santa María Valley, limited to the north by the Cumbres Calchaquíes and tothe south by the Sierra de Aconquija (Figures 2, 3).

The Amaicha valley is narrow, with an average width of about 4 km (Figure 3). The developed piedmonts belong to the southern foothills of the Cumbres Calchaquíes; it is covered by Sequences III and IV of the Santa María Group and the Quaternary alluvial fan deposits (Figure 3; Table 3).

The Tafí del Valle fault had a normal component separating the Sierra de Aconquija from the Cumbres Calchaquíes and forming the Tafí and Amaicha valleys. This fault allowed the deposition of the Tertiary sequence in the Amaicha Valley, resulting from an underdeveloped heritage from the Cretaceous Rift (Mon et al., 2012) (Figures 3, 4). The Tafí del Valle fault probably could have had an incipient development during the Cretaceous Rift stage, which did not prosper.

© 2023 Global Journals

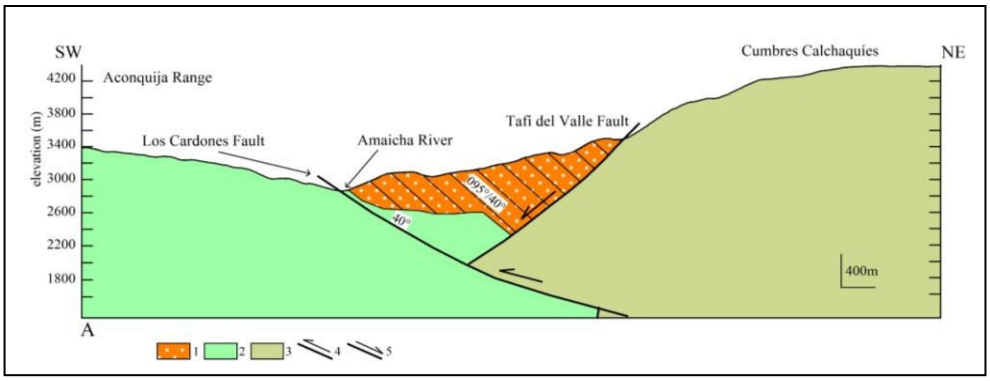


Figure 4: Geological profile A, transverse to the Amaicha Valley. 1: Los Corrales Formation, Santa María Group, Neogene. 2: Paleozoic granite. 3: Proterozoic early - Paleozoic Basement. 4:Reverse fault. 5: Normal fault. The Los Cardones fault zone has a general dip direction to the NE, dipping 40° (Figure 3).

Sediments of Cretaceous or Tertiary age were not yet found in the Tafí valley, possibly because the area remained elevated, until in the lower Tertiary, it began to partially fill up on the Amaicha valley side, reaching the Neogene deposits at the foot of the Infiernillo fault. For example, remnants of the lower Tertiary red sediments (Santa Bárbara Subgroup) occur at the foot of the Los Corpitos and Chasquivil faults (Gutiérrez et al., 2021).

Neogene sedimentary sequences of the Santa Maria Group spread eastward into the Sierra de Aconquija against the dipping ramp to the west, which was later cut by the reverse Infiernillo fault, vergent to the NW (Mon et al., 2012). The Infiernillo fault separated the Amaicha Valley from Tafí Valley. It would have also facilitated the magmatic ascent that originated the vulcanites in the northern zone of the Sierra de Aconquija (Figure 2). The horizontal displacement of the Tafí del Valle fault is affecting the sedimentary sequence of theSanta María Group in the Santa María Valley (Mon et al., 2012).

In the Amaicha River, the plane of the Los Cardones fault was measured (Gutiérrez et al., 2021). It is a reverse fault that dips to the NE. Because the fault plane in the granite outcrops is broken, it was possible to measure a plane dipping 40° to the NE (Figure 4). The Los Cardones fault cuts the Tafí del Valle fault and places the layers of the Los Corrales Formation with a 40° dip to the east (Table 3; Figures 3, 4). Southwest of the Los Cardones fault, the layers of the Los Corrales Formation slope 20° to the SE (Figure 3).

In the Amaicha Valley, tectonic activity is affecting the Quaternary conglomerate sequence. It is possible to see how the layers of the Andalhuala Formation are riding on the Yasyamayo Formation, and the faults also affect the quaternary gravels (Table 3; Figures 3, 5). These faults occur in the central zone of the valley, far from the main faults that limit the mountains.

d) Tafí valley

The Tafí Valley is located at the northeast end of the Sierra de Aconquija, bordered to the north by the Cumbres Calchaquíes. In the valley's centre, the independent relief of Loma Pelada stands out, dividing the valley into two related areas, Las Carreras Valley to the west and Tafí Valley to the east (Figures 2, 3). The bottom of the Tafí Valley is between 1800 and 2300 ma.s.l.,crossed from north to south by the Tafí del Valle River.

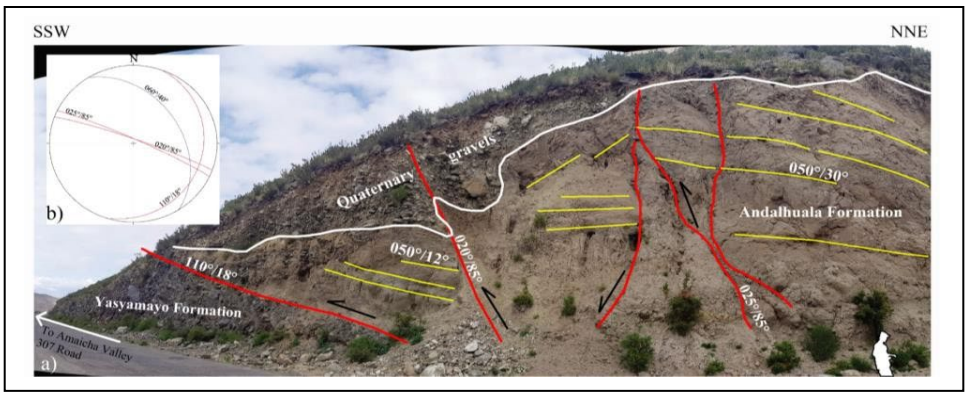


Figure 5: A: Photographic illustration in the Amaicha Valley. A reverse fault places the Andalhuala Formation on the Yasyamayo Formation. Other faults also affect quaternary gravels. The white lines mark the contacts of the sedimentary units. Yellow lines indicate bedding. Red lines identify structures. On the lower right edge, in white, a person's half-length silhouette indicates scale. B: Diagram of resulting fractures represented in Schmidt's equiareal network, lower hemisphere. Los Cardones fault in blue line. In red lines faults in this figure.

© 2023 Global Journals

In the Tafí valley, on the igneous-metamorphic basement (López et al., 2017) rest thick greyish-brown conglomerates, called Lomitas Pegadas Formation (González, 1999), covered by loess from Tafí del Valle Formation (Collantes et al., 1993), dated at 1.15 Ma (Middle Pleistocene) by Schellenberger et al. (2002) (Table 3).

Organic matter contained in lake sediments in the area of El Rincón, Tafí del Valle, was dated with 14C, registering ages between 10,350 ± 80 and 4120 ± 60 a BP (Garralla et al., 2001). Ortíz and Jayat (2007) carried out radiocarbon dating on bone remains found in the Tafí del Valle Formation and located at the Pleistocene-Holocene limit (10.25–9.65 ka cal. BP). Recent studies carried out an evolutionary geomorphological model of the Lateglacial and Holocene accumulations in the valleys, determining four degradation stages dated between 13,000 and 630a BP with 14C, thermo Luminescence, and tephra layers underlying charcoal samples (Peña-Monné and Sampietro-Vattuone, 2018; Sampietro-Vattuone et al., 2019; Sampietro-Vattuone and Peña-Monné, 2016) (Table 3).

Alluvial fans are fed from Cumbres Calchaquíes and Sierra de Aconquija. The deposits corresponding to the Cumbres Calchaquíes are better developed, covering the entire southern edge mountain front and reaching up to 4 km wide. On the other hand, the deposits in the foothills of the Sierra de Aconquija occupy only half of the northern front of the mountain range.

They are 2 or 3 km wide (Figure 3). The thickness of the Quaternary deposits at the Mesada Lamedero is estimated to be about 200 m.

Peña-Monné and Sampietro-Vattuone (2018) defined in Tafí Valley morpho-sedimentary units constituting aggradation phases. Unit H1 represents the oldest hill-side accumulations, riverterraces, and alluvial cones, consisting of well-stratified coarse sands and gravels. Unit H2 occupies a large area constituting alluvial fan deposits made up of sediments similar to H1 (Table 3).

The differential tectonic behaviour of both mountain blocks (Sierra de Aconquija and Cumbres Calchaquíes) generated the segmentation of the NW structures that limit both mountain ranges, the Tafí del Valle fault on the southern edge of the Cumbres Calchaquíes and Los Cardones-Carapunco faults on the edge north of the Sierra de Aconquija (Figures 2, 3). This differential behaviour can be observed in the Los Cardones and Carapunco faults (Figure 3). The Los Cardones fault only has a dip-slip. On the other hand, the Carapunco fault has vertical and horizontal displacement. The Tafí valley reflects a differential tectonic behaviour in neotectonic processes; several zones are distinguished in the foothills of the Cumbres Calchaquíes (Las Tacanas, La Costa II, Los Cuartos, Las Siringuillas, and La Angostura), limited to the west by the Portuguese fault and to the east by the Chasquivil fault (Figure 3).

e) Las Tacanas – El Infiernillo

The Carapunco fault marks the northern limit of the Sierra de Aconquija; the river Tafí del Valle runs through it. The fault begins in the El Infiernillo pass and ends in the La Angostura area (Figure 3). Towards the Tafí del Valle River, the alluvial fans of the Cumbres Calchaquíes and the Sierra de Aconquija converge.

In the Las Tacanas area, it is observed in the satellite images and the geomorphology of the landscape that the alluvial fans of the Cumbres Calchaquíes were reworked and modelled by other processes, different from the accumulation and erosion that characterise these geoforms.

These surfaces are furrowed by deep, parallel, and curved ravines that descend from the Cumbres Calchaquíes and end in the Tafí del Valle River, forming positive reliefs and hills between them (Figures 3, 6). This drainage network with a curved and parallel pattern is represented by deep ravines generated by reverse faults that formed a series of ascending steps tothe NW in the foothills (Figure 6a). In this area, retrograde erosion and landslides on the southern slopes of the streams due to reverse faults that changes the local base level allow evidence of recent tectonic activity.

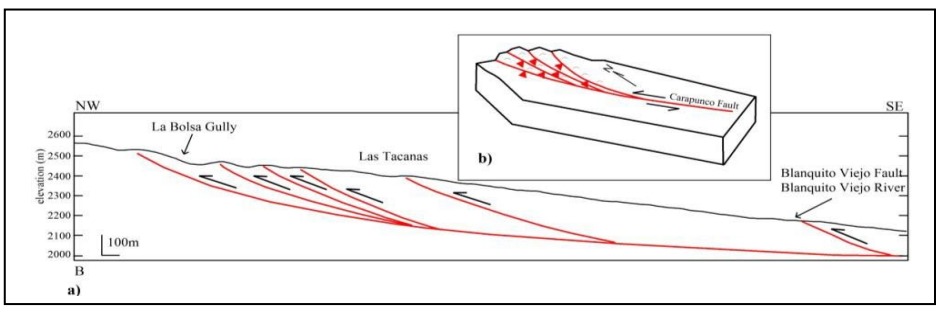


Figure 6: A: Topographic profile B showing the positive relief and the hills formed in the foothills of the Cumbres Calchaquíes, generated by reverse faults, configuring a rough surface limited by deep ravines. B: The plant diagram shows an interpretation of the geometry of interposed contractional fans drawn based on the distribution of the drainage network in Figure 3 and the attitudes of the fault planes.

© 2023 Global Journals

In the upper parts of the foothills, the strata of a sequence of sandy silts, of a light brown colour, with intercalations of conglomerate lenses, with large clasts, maintain an inclination of 18° to the south (Figure 7). Together, these streams and the Tafí del Valle River form an interlaced contractional fan geometry (Figure 6b), like the examples from the literature (Woodcock and Fisher, 1986; Cunningham and Mann, 2007).

This geometry allows us to determine that the Carapunco fault has a sinistral transcurrent component (Figures 3, 6b).

The Cumbres Calchaquíes are exerting pressure on the Sierra de Aconquija, generating the deformation of the foothills of the valley in such a way that the foothills of the Cumbres Calchaquíes are higher than the foothills of the Sierra de Aconquija (Figure 8a). This tectonic process that generates a characteristic morphology and a typical structural geometry is evidenced in the Mesada Lamedero (Figure 8). There, a positive relief structure is formed by the Carapunco and Blanquito Viejo reverse faults, arranging the conglomerate layers of the alluvial fans of the Cumbres Calchaquíes with strong east and west dips (Figures 3, 8b, 9).

Figure 8 shows the ravine raised on the left bank of the Tafí del Valle River. On the right bank of the Blanquito Viejo river, the river terrace comprises light brown sandy silts, with intercalations of conglomerate lenses at the base, passing into a fanglomerate in the upper half of the profile. The conglomeratic lenses dip 30° to the west (265°/30°), a product of the activity of the Blanquito Viejo fault (Figures 8, 9).

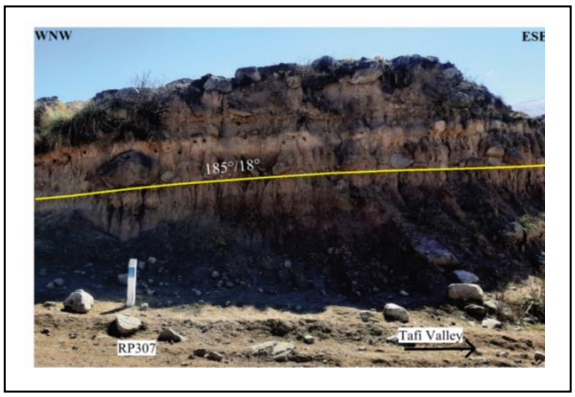


Figure 7: Stratigraphic sequence of the foothills on the right bank of the La Bolsa ravine. The conglomerate strata slope south (185°/18°).

In the Infiernillo, where the Tafí del Valle River is born, the Carapunco Fault can be seen (Figure 10). In some sectors, the fault lays out the metamorphic basement on granitic rocks and sometimes cuts through the granitic rocks (Figure 10a). The Carapunco Fault, with a 40° dip in a NE direction, arranges the Cumbres Calchaquíes on the Sierra de Aconquija (Figure 10b).

f) La Costa II, Los Cuartos

These zones are in the southeast end of the Tafí Valley, where the Tafí del Valle and Chasquivil faults converge (Figure 3). In this area, the Loma Pelada constitutes a positive element that divides the Tafí Valley (Figure 3). The foothill deposits of the Sierra de Aconquija are better developed in the Las Carreras Valley but not on the eastern edge of the Loma Pelada, which is where the piedmonts deposits of the Cumbres Calchaquíes will end up, against the Tafí del Valle River (Figure 3).

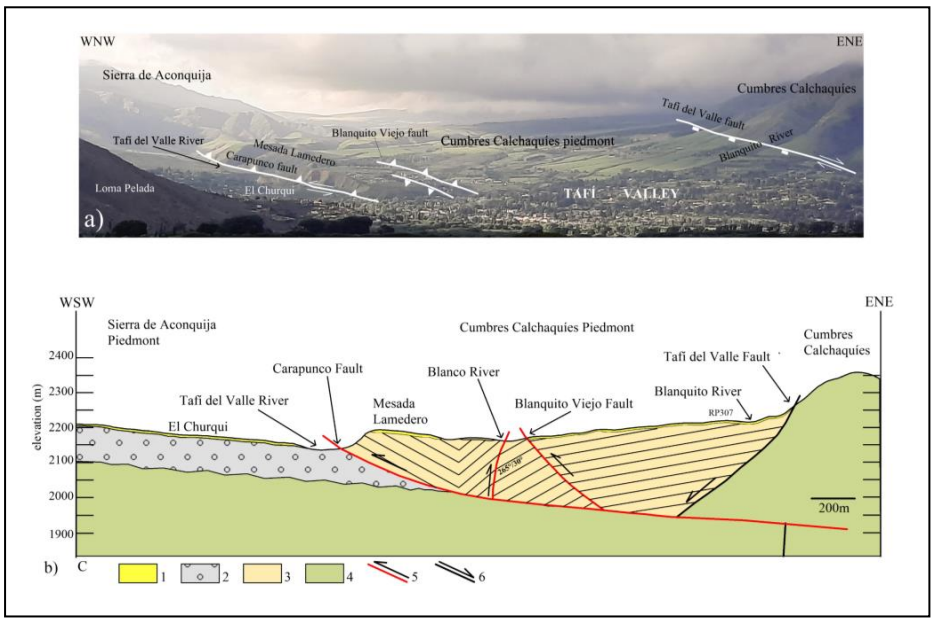


Figure 8: A: Panoramic view of the Tafí Valley tectonics morphology displayed in Figure b. Wecan see the topographic relief of the alluvial fans disturbed by the reverse faults generating the counter slope. It is also observed how the piedmonts of the Cumbres Calchaquíes rise above the Sierra de Aconquija piedmonts through the Carapunco fault. B: C topographic profile showing the

© 2023 Global Journals

Mesada Lamedero positive relief structure formed by the Carapunco and Blanquito Viejo faults. It is observed that the foothills of the Cumbres Calchaquíes are raised and folded over thefoothills of the Sierra de Aconquija. 1: Loess deposits (Q). 2: Alluvial fan deposits (Q). 3: Alluvial fan deposits (Q). 4: Proterozoic basement. 5: Recent reverse faults. 6: Normal fault.

Quaternary structures were generated in the foothills and the mountain front of the Cumbres Calchaquíes (Figure 3). The deformation of the alluvial fans adequately reflects neotectonic activity (Figure 11).

In the La Costa II área, the tectonic deformation of the Quaternary sediments occurs on the mountain front. Here we can see the cuspid zone of the deformed dejection cones, ridden by a metamorphic basement, through a reverse fault dipping to the ENE (080°/80°) (Figure 3).

This fault corresponds to a reactivation of the Tafí del Valle and Chasquivil faults, and the quaternary sediments would be represented by the H1 accumulations (Peña-Monné and Sampietro-Vattuone, 2018) (Figure 3). Other reverse faults (130°/88°, 280°/50°, 115°/80°), measured in the metamorphic basement, also affect the quaternary sedimentary sequence. One ofthese faults (045°/90°) coincides with the Tafí del Valle fault (Figure 3). Here, the quaternary faults affect the accumulations identified as H1, dated by Peña-Monné and Sampietro-Vattuone (2018) between ca. 13000 and 4200 a BP(Figure 3; Table 3).

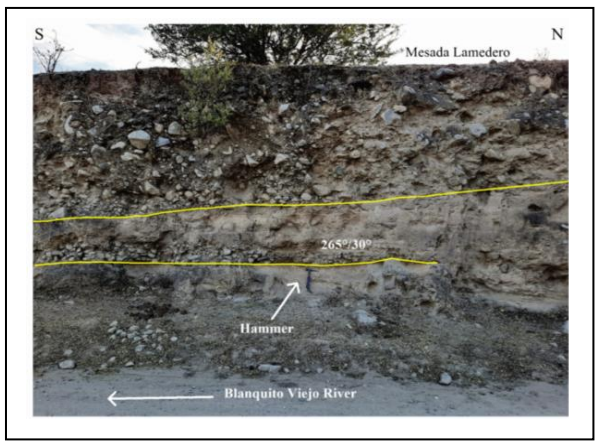


Figure 9: Quaternary terrace on the right bankof the Blanquito Viejo River. The Blanquito Viejo fault affected the sequence, disposing of the conglomerate strata with a west dip (265°/30°).

In this area, rock falls by the terraces' destruction on the ravines' margins are also observed, which allows evidence of recent tectonic activity. The discrete deformation associated with the recent seismic activity recorded in the area generates these neotectonic indicators.

Between the Los Cuartos and Las Siringuillas area, the piedmont landscape is crossed by structures with NW and NE strikes and disturbed by hills of about 400 to 800 m in length and 140 m in width, with NNW strike (Figures 3, 11). These hills comprise Pleistocene sediments, deforming the H1 and H2 accumulations (Figure 11, Table 3). Two anticline fold structures are observed, with NW and NE strikes, which dispose of the Pleistocene conglomerate strata dipping to the NE, SW, and SE, NW, respectively (Figures 11, 12; Table 3).

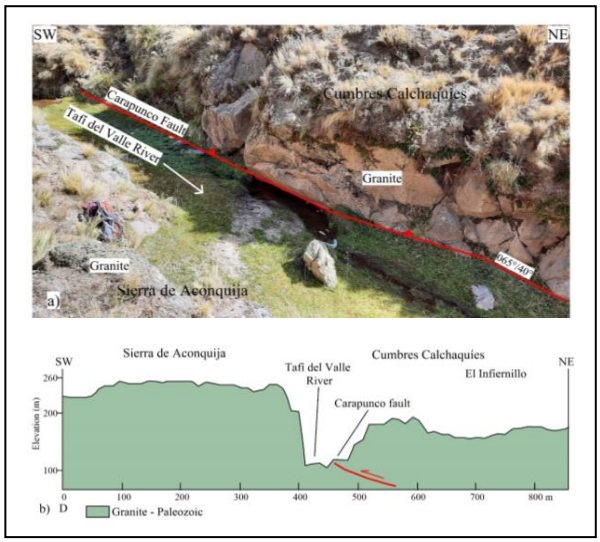


Figure 10: The Carapunco Fault cuts granitic rocks with a 40° dip in a NE direction. It disposes of the Calchaquíes Summits on the Sierra de Aconquija.

The faults have reverse displacement, dipping to the NW and NE (300°/45°, 080°/80°, 125°/70°, 115°/85°, 060°/84°). One of them (060°/84°) also evidenced dextral transcurrent movement, dividing one of the hills and generating a typical whale-back structure and a fault gap. Other structures affect the folds and H1 and H2 accumulations (Figure 12; Table 3) (Gutiérrez et al., 2021).

The faults generated between Los Cuartos are found in the cuspid part of the alluvial fans near the mountain front and generate anticline folds in the Pleistocene deposits (Figures. 11, 12; Table 3). These structures and associated morphologies appear closely related to the Chasquivil fault. The layers of the H2 accumulations, dated by Peña-Monné and Sampietro-Vattuone (2018)between ca. 4200–630 to BP, are also affected by tectonic activity (Figure 12a). The drainage network also shows tectonic activity. The anticline structures interrupt and divert the channels, showing recent incisions in the H2 accumulations (Figures 11, 12).

g) Ambato Block

The morphology of the tectonic depression Las Estancias - Campo del Pucará represents an inverted alluvial fan, and the morphotectonics of the north end of the Ambato Block evidence tectonic processes of counterclockwise rotation (Figure 2) (Gutiérrez, 2000; Gutiérrez and Mon, 2008). The northern end of the Ambato Block evidences a break, marked by the Tucumán Lineament and the Las Cañas River, representing structures oblique to the Andean strike.

© 2023 Global Journals

The deformation processes are active (Gutiérrez et al., 2019).

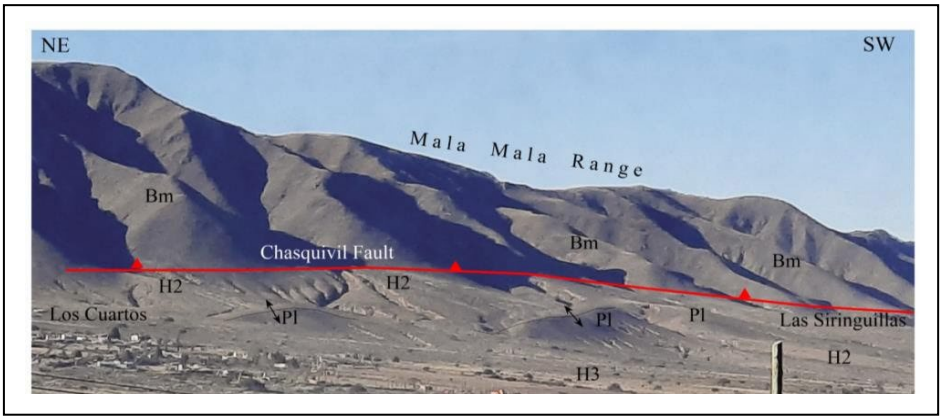


Figure 11: Photo shows the piedmont deformation by neotectonic processes associated with the Chasquivil fault. Hills oriented to the NNW are observed, made up of Pleistocene sediments, modifying the course of surface drainage and disturbing the H2 accumulations. Symbols indicateanticlinal folds.

As part of the geotechnical works in the northern end of the Ambato Block, the company MAA (Minera La Alumbrera S.A.) keeps a continuous record of the displacements of some fractures in the igneous-metamorphic basement (Figure 13a). These fractures have a high degree of dip (145°/70° - 040°/85°). To measure the displacement of some fractures, the company placed gauges that measure movement on three orthogonal axes (A, B, C) (Figure 13b). On axis A, the horizontal separation of the gauge plates is measured in the centre of the overlap zone, parallel to the fracture plane (Figure 13). On the B axis, the horizontal distance between the tips of the gauge plates is measured (Figure 13).

The C axis measures the vertical movement of the fracture. It is the distance between the smaller plate's lower edge and the larger plate's upper edge, measured at the centre of the overlap (Figure 13). A third axis, D, was added to obtain the resulting displacement of B and C (Figure 13a). The measurement uses a digital calliper, achieving an acceptable accuracy of ±1mm.

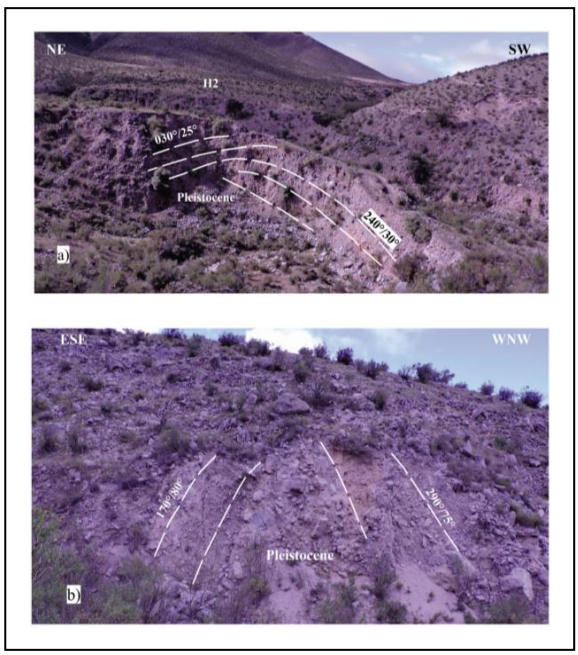


Figure 12: View of folds in the foothills; the folded strata correspond to the Lomitas PegadasFormation. A: Anticline NW strike. B: NE direction fold whose strata show a strong dip.

The company MAA provided the data obtained month by month for 2021 and 2022.

Figure 13a marked the fractures' direction and sense of displacement according to axes A, B, and C. The measurement obtained in B (Figure 13b) also represents a horizontal displacement perpendicular to the fracture plane (Figure 13a). The measurement obtained in C (Figure 13 b) represents the vertical displacement on the fracture plane (Figure 13a). In Figure 13a, arrow D indicates the direction and sense of displacement resulting from the movements in axes B and C.

The Pythagorean theorem (Eq. (2)) was applied to obtain the resultant D:

$$D=(D^2 = B^2 + C^2). \quad (2)$$

© 2023 Global Journals

From the reading obtained between 2021 and 2022, it is interpreted that the measurements obtained in the different months are variable. The minimum and maximum measurements can determine an average annual displacement. For 2021, the average displacement in the A axis was 0.74 mm/y and for the D axis, 2.55 mm/y. For 2022, the average displacement of the A axis was one mm/y and for the D axis, 2.6 mm/y.

V. Santa Bárbara System

The southernmost end of the Sub-Andean System, south of the Juramento River, is represented by low mountains with few outcrops. The best outcrops occur on the Colorado, Cantero, and Remate hills and the flanks of the La Candelaria, Medina, and del Campo range(Figure 14) (Mon and Gutiérrez, 2007).

Intensely micro-folded low-grade Proterozoic schists form the basement outcrops in the La Candelaria, Medina, del Campo, and La Ramada ranges (Figure 14). Some pink quartzites areattributed to the Cambrian age on the western flank of the La Candelaria range (Ricci and Villanueva, 1969).

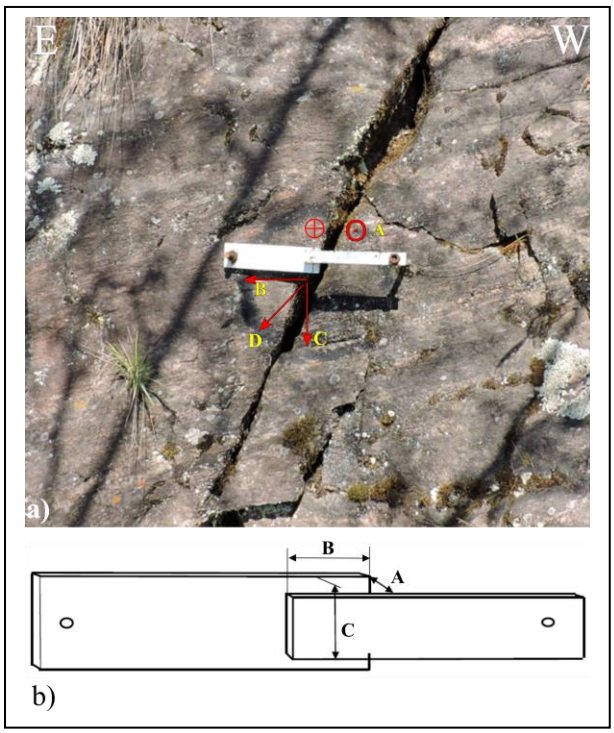


Figure 13: A: Photograph illustrating the gaugeanchored to the fracture to measure displacements in three perpendicular axes. On the fracture, the direction of the displacements is indicated with symbols in red for the measurements of A, B, and C. The circles represent the tip and the tail of an arrow that indicate the direction of displacement. B: Diagram of the meter and the measurements made in three orthogonal axes.

Jakúlica (1948) mentions layers of green and whitish shale from the Ordovician period below white and pink quartzites attributed to the Devonian, at the bottom of an open pit excavation, at Puesto La Aguada, south of Cerro Colorado (Figure 14). These Devonian quartzites also crop out in the anticline cores of the Cantero and Remate hills (Mon and Gutiérrez, 2007). The stratigraphic sequence north of the oblique fault that marks the southern end of the Cerro Colorado range (Figures 14, 15) contains thick Cretaceous sequences of the Salta Group (Mon and Gutiérrez, 2007) (Figure 15). To the south, a few shallow outcrops occur on the western flank of the La Candelaria range and in the Río Nío Valley, proving that the Neogene layers of the Anta Formation sit directly on the Paleozoic (Figure 14). The Quaternary deposits formed by old terraces of the Juramento River are conglomerates with limestone and quartzite boulders of thin thickness; they are tilted to the west with dips greater than 5° (Mon andGutiérrez, 2007).

At the southernmost segment of the Sub-Andean System (Figure 14), which extends for 100 km in the Andean foreland, the basement participates in deformation as in the La Candelaria, Medina, del Campo, and La Ramada ranges (Mon and Gutiérrez, 2007). This set of mountains reaches maximum heights of 2,400 m a.s.l. in the La Candelaria Range. To the east of this mountain range and south of the Juramento River (Figure 14), the most prominent outcrops coincide with Cerro Colorado, which, at its highest point, reaches 1,000 m a.s.l. It continues to the south, a cord of low mountains, with few outcrops, covered by scrub and thorny scrub, in the outermost part of the Andean foreland, where most of the structures are sub-outcrops, only glimpsed in satellite images.

The Andean deformation folded this set of sierras against the faulted edge of the Chaqueña Plain, generating bowing and displacement of the folds (Figure 14, 15). In the Metán basin, the folds and structures are covered by a thick sedimentary sequence of more than 7,000 m thick, only visible in seismic profiles (Mon et al., 2005; Iaffa et al., 2011). In the Choromoro Valley, the folds and structures are also covered, but the sedimentary sequence is not as thick. Therefore, the morphology of the folds is visible in the radar images (Figure 14). The Neogene structures affecting Quaternary deposits are best developed in the La Candelaria range (Gutiérrezet al., 1997) (Figure 14).

The geometry of the Neogene faults was determined on both flanks of the La Candelaria range. This fault geometry was determined by making profiles with 2D electrical resistivity tomography, seismic methods, and digital terrain models prepared with drone images (Aranda-Viana et al., 2017; Arnous et al., 2020).

Repeated offsets during moderate to large earthquakes in the Quaternary are the most likely origin for these scarps, which suggests recurrent, spatially disparate seismogenic quaternary deformation processes in the broken foreland (Aranda-Viana et al., 2017; Arnous et al., 2020).

© 2023 Global Journals

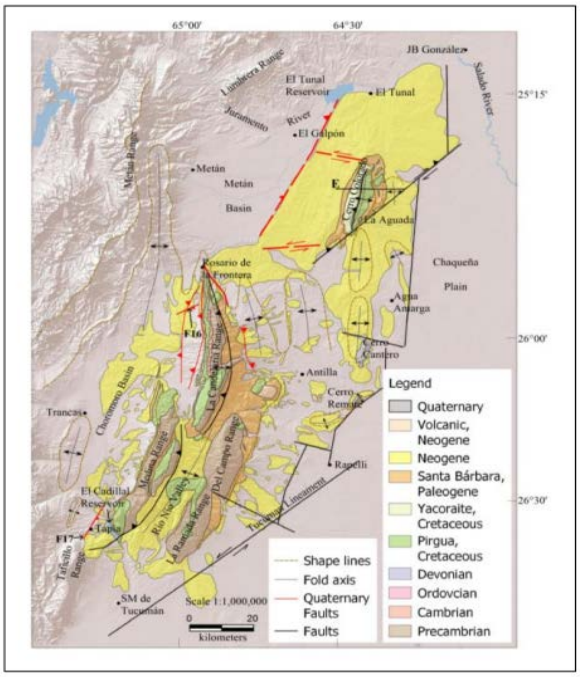


Figure 14: Map of the Santa Barbara System. F16: Figure 16 location. F17: Figure 17 location. Fold contour shape lines were drawnprimarily to indicate the location of buried folds. These lines also allow us to see the curved geometry that the folds acquire due to neotectonic deformation. Dashed red lines indicate blind faults, showing activity without surface expression (Zeckra, 2020).

Some faults are blind, riding quaternary alluvial fans. In Figure 16, the conglomeratic strata and silty deposits are affected by blind faults. The fault dips 30° SE. It is interesting to observe the curved morphology of the terrace surface, which accompanies the displacement of the fault (Figure 16). This curved geometry is also observed in the images of remote sensors in several sectors on the flanks of the La Candelaria range, evidencing that blind faults produce them.

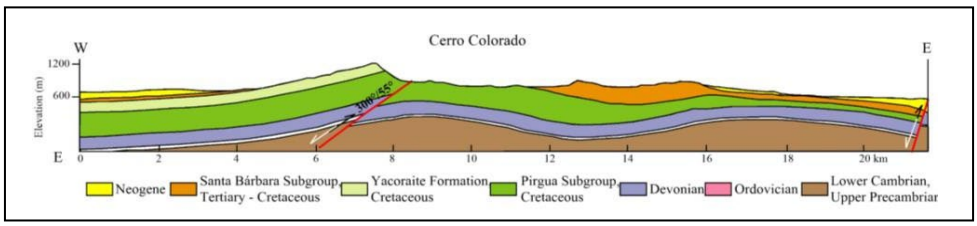


Figure 15: Profile of Cerro Colorado. The complete stratigraphic sequence representing theSanta Bárbara System is shown.

To the north of the Taficillo range, a stratigraphic sequence of the Río Salí Formation of the Miocene age is cut by a thrust fault (Figure 17). The strata are gently folded, dipping to the NE, between 25° and 30°. The fault dips 40° to the SE. A microfold of the strata is observed at itsbase, and in the upper part, the fault affects Quaternary deposits. Other conjugate reverse faults are generated on the left side of the main fault, which also affects the Quaternary deposits. Towards the left side of the outcrop, a normal fault causes a slip of the Quaternary deposits(Figure 17).

VI. Chaqueña Plain

This extensive sedimentary basin extends from the eastern edge of the Santa Bárbara System and Sierras Pampeanas (Figure 1) to join the Paraná basin to the east (Pezzi and Mozetic, 1989). Neotectonic deformation did not bring the stratigraphic sequence that fills it to the surface buried by Quaternary deposits. Its geological history is known and interpreted through information from oil wells, seismic lines and magnetotelluric profiles.

Between the Upper Precambrian and the Silurian, an extensional tectonic event occurred that would be associated with a shear system of significant vertical displacement that affects the crystalline basement and originates basins like Las Breñas fault and its homonymous half- graben, inverting towards the upper Plaeozoic giving rise to the Pampeano-Chaqueño arch (Chebli et al., 1999) (Figures 1, 18). Based on both the geotectonic context and the magnetotelluric results, it conjectured that the sharp lateral discontinuity observed at both sides of the Pampeano-Chaqueño arch in the resistivity model represents the boundary between the Río de la Plata craton and the Pampean terrane or another Precambrian cratonic fragment (Pomposiello et al., 2010).

© 2023 Global Journals

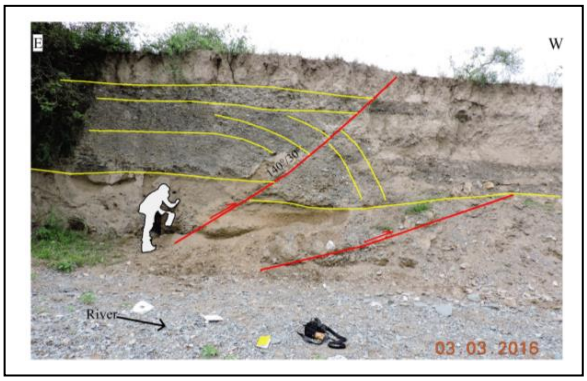


Figure 16: River terrace faulted on the left bank of a river. Location in Figure 14. With yellow lines, the strata are delimited. The red lines mark the faults. Fault data indicates dipdirection/dip.

The Otumpa hills, limited to the east by the Otumpa Lineament (Rossello and Veroslavsky, 2012) (Figure 1), are the surface expression of the Pampeano-Chaqueño arc and constitute a Gondwanan relict morphostructure, with Mesozoic and Cenozoic reactivations (Peri, 2012). The geometry of the subsoil structures in this zone, interpreted through seismic profiles, shows high-angle reverse faults and asymmetric and symmetric folds, revealing tectonic inversion processes (Peri, 2012; Rossello and Veroslavsky, 2012). The Otumpa hills (Figure 1) are mainly linked to an antiform of about 150 kilometres of wavelength originated by double tectonic vergence (Peri, 2012).

According to the isopach map (Chebli et al., 1999) and the magnetotelluric profile (Pomposiello et al., 2010), the Lower Paleozoic basins developed to the west and east of the Pampeano-Chaqueño arc (Figure 19).

The superficial expression of neotectonics is reflected by the paleochannels transversal to the Otumpa hills and by the wedges of the Cenozoic sequences observed in the seismic lines.

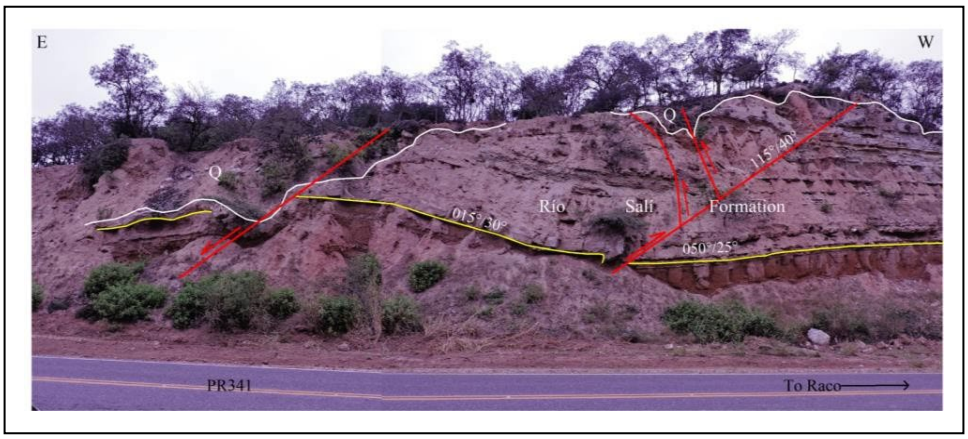


Figure 17: Outcrop of the Río Salí Formation (Miocene) on Provincial Route 341 (PR341). Withyellow lines, the strata are delimited. The red lines mark the faults. White lines mark the contact between the Río Salí Formation and the Quaternary. Fault data indicates dip direction/dip.

These paleochannels, with a W-E strike, represent the primitive direction of the surface runoff of the Salado River. Neotectonic processes diverted runoff from the Salado River to its current course in an N-S direction (Peri and Rossello, 2010) (Figure 1).

The deep seismicity of the Chaco Plain-aligned N-S (Figure 1) was linked to the depth ofthe Pacific slab (Peri, 2012). Our interpretation connects this surface seismic expression with a blind, sub-vertical structure called El Hoyo Lineament (Figures 1, 19). The neotectonic reactivation of the El Hoyo and Otumpa lineaments gave rise to the Otumpa hills and the diversion of surface runoff.

VII. Discussion

The NE compression due to the convergence of the Nazca and South American plates produces deformation through movement in faults of diverse geometries. The deformation is influenced, among other things, by the rheology of the rocks and pre-existing faults (Ikeda, 1983; Iaffa et al., 2011; Gutiérrez et al., 2019; Gutiérrez and Mon, 2008; Riller and Oncken, 2003; Rodgers and Rizer, 1981; Zampieri et al., 2012). Seismic rupture occurs when the elastic stress towhich the rock is subjected exceeds its frictional resistance (Sibson, 1982; Nortje et al., 2011; Kamb et al., 1971; Ikeda, 1983).

© 2023 Global Journals

Most earthquakes recorded in the study area are of magnitude 3 and 5. These earthquakes occur in the Andean foreland between the first 70 km depth. Earthquakes of magnitude >6 occur less frequently, between 0-33 km and 500-600 km depth (Figure 1; Table 2).

The convergence of NE-directed tectonic plates leads to continuous tectonic deformation of the central Andes in Argentina. Those active tectonics migrated eastward from the Puna since the middle Eocene (Del Papa et al., 2005; Deeken et al., 2006; Carrapa and De Celles, 2015). In the Miocene, it reached the western edge of the Eastern Cordillera (Jordan and Alonso, 1987; Starck and Vergani, 1996; Carrera and Muñoz, 2008; Carrapa et al., 2011; and Pearson et al., 2013). The thick conglomeratic deposits of Pliocene-Pleistocene age on the slopes of Cumbres Calchaquíes, Sierra de Aconquija, Velazco range, Cerro Pampa (Gutiérrez et al., 2003; Gutiérrez et al., 2023; González, 1999) show active tectonics of considerable magnitude. The Lomadas de Otumpa originate in Paleozoic tectonic events, with repeated reactivations of pre-existing structures during Andean tectonics, currently causing the diversion of the surface drainage network (Peri, 2012).

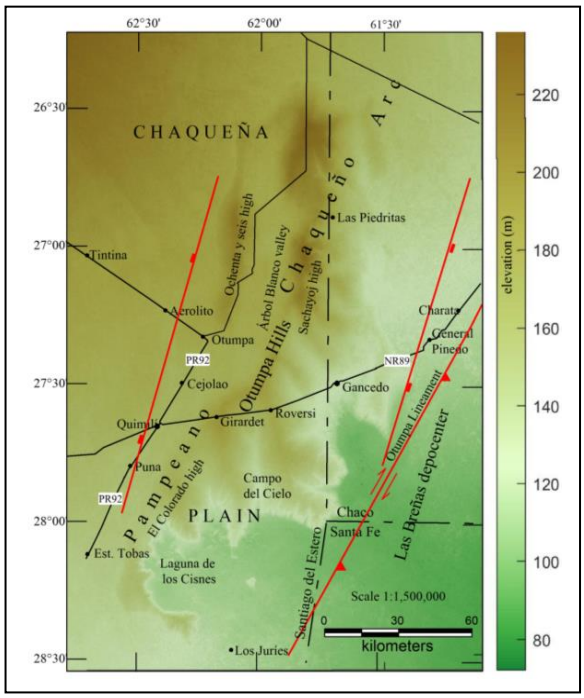


Figure 18: Map image that represents the positive relief of the Otumpa Hills.

Records of neotectonic deformation (Pleistocene-Holocene) in the Andean foreland indicate values between 0.3 to 11 mm/yr (Pearson et al., 2013; McFarland and Bennett, 2017; Echavarria et al., 2003; García et al., 2013; García et al., 2019; Ramos et al., 2006). This work provides data on displacements in basement fractures of 0.74 - 2.6 mm/yr (2021 and 2022). Zeckra (2020) discovered high seismic activity confined along the Andean thrust front with a magnitude of completion MC 1.45 along steep and deep thrust faults generated through the inversion of Cretaceous normal faults.

The thick conglomeratic deposits such as the Yasyamayo (Pliocene) and Lomitas Pegadas (Pleistocene) formations (Figures 5, 12; Table 3) record the last tectonic events of considerable magnitude for the region. Since then, neotectonic deformation appears to have slowed down (Pearson et al., 2013; McFarland and Bennett, 2017; Echavarria et al., 2003, García et al., 2013; García et al., 2019; Ramos et al., 2006).

Considering these deformation values, the neotectonic deformation observed in the outcrops (faults, folds and diversion of the drainage network), and the evidence of the seismic profiles, it is possible to interpret that the seismic activity in the study area from the Pleistocene to the present, remained between the current records (Figure 1; Table 2). This seismic activity, sustained over time, is sufficient to produce deformation in the foothills (Figures 11, 12, 14, 18), reactivate pre-existing faults with small displacements (Figures 5, 8, 17) and generate minor new faults in recent conglomeratic deposits (Figure 16). Many faults are blind. However, the deformation of the landscape and the modification of the drainage network are direct indicators of the activity of these structures.

VIII. Conclusions

The neotectonic deformation occurred in the foothills of the Cumbres Calchaquíes, La Candelaria,

© 2023 Global Journals

and Taficillo ranges through folds and fractures. Some fractures experienced horizontal movements, and others had reverse displacements, retrovergent to the Andean deformation (Figures 3, 5, 6, 8, 11, 12, 14, 16, 17). Tectonic activity in the piedmont of Cumbres Calchaquíes is affecting deposits dated 630 a BP.

Other manifestations of neotectonic activity are observed in the Santa Bárbara System (Metán, Choromoro basins and east of the La Candelaria range) and Llanura Chaqueña (Figures 1, 14). In the Metán basin, reactivations of Cretaceous fractures are observed in the seismic profiles and on the surface, the deviation of the drainage network. Eventual earthquakes of greater magnitude, such as El Galpón, produce ruptures on the surface. In the Choromoro basin, the landscape appears undulating due to subsoil folds buried by Quaternary deposits that are beginning to be shaped (Figure 14), and new blind faults break the strata of the fluvial terraces (Figure 16). The Colorado, Cantero and Remate hills are folded and folded to the east of the La Candelaria range. Cerro Colorado is the highest expression of the complex. The folds insinuate to the south in the landscape, covered by Quaternary deposits (Figure 14). In the Chaqueña Plain, the subtle uplift of the Lomadas de Otumpa generates control and diversion of the surface drainage network (Figure 1).

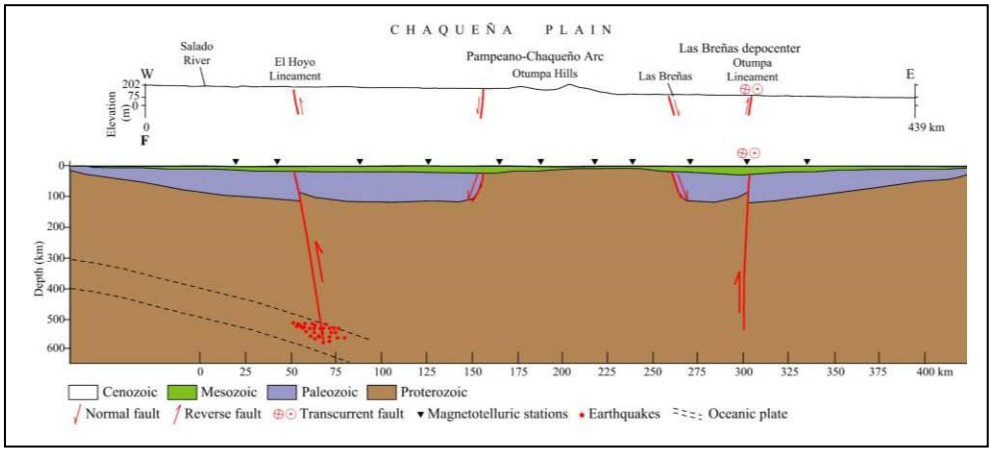


Figure 19: A: Topographic profile of the Chaco Plain. The vertical scale is exaggerated to illustrate the positive relief of the Otumpa Hills. The location of the profile is shown in Figure 1. The profile coincides with the trace of the magnetotelluric stations (Pomposiello et al., 2010) (Figure 1). B: Profile modified from (Pomposiello et al., 2010). To interpret the structures and the stratigraphic sequence in-depth, we have taken the works of (Cristallini et al., 2004; Pezzi and Mozetic, 1989; Chebli et al., 1999; Pomposiello et al., 2010; Peri (2012); Rossello and Veroslavsky, 2012) as a basin.

In the study region, many earthquakes coincide with regional lineaments and faults (Tafí del Valle, Chasquivil, Río Muerto, Los Pinos, Los Hoyos). This coincidence shows these regional faults are active (Figures 1, 2). The seismic activity in the study area from the Pleistocene to the present remained between the current records. It sustained over time is sufficient to produce folds, new faults and reactivation of pre-existed faults in materials of low cohesion.

Acknowledgements

This work was carried out with the support of the National University of Tucumán and the financing of the Argentine-German University Center. My thanks to Minera La Alumbrera S.A. for logistical support and for providing me with geotechnical data. Thanks also to the anonymous reviewers for their suggestions and contributions.

Declarations

Conflict of interest on behalf of all authors, the corresponding author states that there is no conflict of interest.

References Cited

1. Abascal, L.V., 2005, Combined thin-skinned and thick-skinned deformation in the central Andean foreland of northwestern Argentina: Journal of South American Earth Sciences 19: p. 75–81.
2. Aceñolaza, F.G., and Toselli, A.J., 1981, Geología del noroeste argentino: Publicación especial N° 1287 de la Facultad de Ciencias Naturales e IML, Universidad Nacional de Tucumán, Argentina, 212 p.
3. Allen, J.L., and Shaw, C.A., 2011, Seismogenic structure of a crystalline thrust fault: fabric anisotropy and coeval pseudotachylyte-mylonitic pseudotachylyte in the Grizzly Creek Shear Zone, Colorado: In: Fagereng A, Toy VG, Rowland JV (eds) Geology or the earthquake source: a volume in honour of Rick Sibson. Geological Society, v. 359. Special Publications, London, p. 135–151.
4. Ambraseys, N.N., and Tchalenko, J.S., 1969, The Dasht-e-Bayaz (Iran) earthquake of August 31, 1968: a field report: Bull Seismol Soc Am 59: p. 1751–1792.

© 2023 Global Journals

5. Aranda-Viana, R.G., Bianchi, C., Aramayo, A., Alvarado, L., Arnous, A., Hongn, F., and Strecker, M., 2017, Modelo de imágenes y fotogrametría de la escarpa occidental de la Sierra de la Candelaria con el uso de vehículo aéreo no tripulado: Actas XX Congreso Geológico Argentino, Tucumán 201, Abstracts, 15 p.
6. Arnous, A., Zeckra, M., Venerdini, A., Alvarado, P., Arrowsmith, R., Guillemoteau, J., Landgraf, A., Gutiérrez, A.A., and Strecker, M.R., 2020, Neotectonic Activity in the Low-Strain Broken Foreland (Santa Bárbara System) of the North-Western Argentinean Andes (26°S): Lithosphere, Article ID 8888588, 25 p.
7. Bossi, G.E., Georgieff, S.M., Gavriloff, I.J.C., Ibáñez, L.M., and Muruaga, C.M., 2001, Cenozoic evolution of the intramontane Santa María basin, Pampean Ranges, northwestern Argentina: Journal of Sputh American Earth Sciences 14: p. 725–734.
8. Brace, W., and Byerlee, J.D., 1966, Stick-slip as an earthquake mechanism: Science 153: p. 990– 992.
9. Butler, R.F., Marshall, L.G., Drake, R.E., and Curtis, G.H., 1984, Magnetic polarity stratigraphy and 40K-40Ar dating of late Miocene and early Pliocene continental deposits, Catamarca Province, NW Argentina: Journal of Geology 92(6): p. 623–636.
10. Carrapa, B., and De Celles, P.G., 2015, Regional exhumation and kinematic history of the Central Andes in response to cyclical orogenic processes: Geological Society of America Memoirs 212: p. 201–213. https://doi.org/10.1130/MEM212.
11. Carrapa, B., Trimble, J., and Stockli, D., 2011, Patterns and timing of exhumation and deformation in the Eastern Cordillera of NW Argentina revealed by (U-Th)/He thermochronology: Tectonics 30, TC3003. https://doi.org/10.1029/2010TC002707.
12. Carrapa, B., Adelmann, D., Hilley, G.E., Mortimer, E., Sobel, E.R., and Strecker, M.R., 2005, Oligocene range uplift and development of plateau morphology in the southern Central Andes: Tectonics 24(4), TC4011. https://doi.org/10.1029/2004TC001762.
13. Carrera, N., and Muñoz, J.A., 2008, Thrusting evolution in the southern Cordillera Oriental (northern Argentine Andes): constraints from growth strata: Tectonophysics 459(1-4): p. 107–122. https://doi.org/10.1016/j.tecto.2007.11.068.
14. Chebli, G.A., Mozetic, M.E., Rossello, E.A., and Bühler, M., 1999, Cuencas sedimentarias de la Llanura Chacopampeana: Instituto de Geología y Recursos Minerales, Geología Argentina, Buenos Aires, Anales 29(20): p. 627–644.
15. Collantes, M.M., Powell, J., and Sayago, J.M., 1993, Formación Tafí del Valle (Cuaternario superior), provincia de Tucumán (Argentina): litología, paleontología y pleoambientes: XII Congreso Geológico Argentino y II Congreso de Exploración de Hidrocarburos, Actas II, Abstracts, p. 200–206.
16. Costa, C.H., 2000, Geomorphic signature of Quaternary deformation and strategies for regional mapping in Argentina: In: Proceedings world active faults symposium, 31° International Geological Congress, Brazil, Abstract, CD-Rom.
17. Costa, C.H, Ahumada, E.A., Gardini, C.E., Vázquez, F.R., and Diederix, H., 2014, Quaternary shortening at the orogenic front of the Central Andes of Argentina: the Las Peñas Thrust System: In: Sepúlveda SA, Giambiagi LB, Moreiras SM, Pinto L, Tunik M, Hoke GD, Farías M (eds) Geodynamic processes in the Andes of Central Chile and Argentina. Geological Society, v. 399. Special Publications, London, 21 p.
18. Costa, C.H., 2019, La migración del frente de corrimiento neotectónico de las Sierras Pampeanas y su impronta morfológica: Revista de la Asociación Geológica Argentina 76(4): p. 315– 325.
19. Cristallini, E.O., Comınguez, A.H., Ramos, V.A., and Mercerat, E.D., 2004, Basement double-wedge thrusting in the northern Sierras Pampeanas of Argentina (27°S)- Constraints from deep seismic reflection: In: K.R. McClay (ed) Thrust tectonics and hydrocarbon systems, vol 82. AAPG Memoir, p. 65–90.
20. Cunningham, W.D., and Mann, P., 2007, Tectonics of strike-slip restraining and releasing bends: Geological Society Special Publication N° 290, London, p. 1–12.
21. Deeken, A., Sobel, E.R., Coutand, I., Haschke, M., Riller, U., and Strecker, M.R., 2006, Development of the southern Eastern Cordillera, NW Argentina, constrained by apatite fission track thermochronology: From Early Cretaceous extension to Middle Miocene shortening: Tectonics 25, TC6003. https://doi.org/10.1029/2005TC001894.
22. Del Papa, C., Hongn, F.D., Mon, R., Powell, J., and Petrinovic, I., 2005, Stratigraphy and syndepositional structures of the basal foreland deposits in the northern valley Calchaquí, NW Argentina: 6th International Symposium on Andean Geodynamics, Barcelona, Extended Abstracts, p. 215–217.
23. Echavarria, L., Hernández, R., Allmendinger, R., and Reynolds, J. 2003, Subandean thrust and fold belt of northwestern Argentina: Geometry and timing of the Andean evolution: American Association of Petroleum Geologists Bulletin 87(6): p. 965–985. https://doi.org/10.1306/01200300196.
24. Fagereng, A., and Toy, V.G., 2011, Geology of the earthquake source: an introduction. In: Fagereng A, Toy VG, Rowland JV (eds) Geology or the earthquake source: a volume in honour of Rick Sibson: Geological Society. London, Special Publications, p. 1–16.

© 2023 Global Journals

25. Figueroa-Villegas, S., Escalante, L., Hongn, F., and Strecker, M., 2017, Deformación tectónica Holocena en la transición entre las Sierras Pampeanas y Cordillera Oriental, valle de Cafayate (26°00' - 25°50' Lat., 66°00' - 65°50' Long.), Salta, Argentina: Actas XX Congreso Geológico Argentino, Sesión Técnica 2, Geología estructural y geotectónica, Abstracts, p. 62–67.
26. García, V.H., Hongn, F.D., Yagupsky, D., Pingel, H., Kinnaird, T., Winocur, D., Cristallini, E., Robinson, R., and Strecker, M.R., 2019, Late Quaternary tectonics controlled by fault reactivation. Insights from a local transpressional system in the intermontane Lerma valley, Cordillera Oriental, NW Argentina: Journal of Structural Geology 128, 103875. https://doi.org/10.1016/j.jsg.2019.103875.
27. García, V.H., Robinson, R.A., Hongn, F.D., Cristallini, E.O., Yagupsky, D.L., Winocur, D., and Vera, D.R., 2013, Late Quaternary uplift rate of Lomas de Carabajal, Lerma valley, Cordillera Oriental, NW Argentina. Insights from structural analysis and OSL dating: Actas CD, Aachen, Alemania: 4th International INQUA Meeting on Paleoseismology, Active Tectonics and Archeoseismology, Actas, Abstracts, CD, Aachen, Alemania.
28. Garralla, S., Muruaga, C., and Herbst, R., 2001, Lago El Rincón, Holoceno del departamento de Tafí del Valle, provincia de Tucumán (Argentina): palinología y facies sedimentarias: Publicación especial-Asociación paleontológica Argentina, Argentina, p. 91–99.
29. Georgieff, S.M., and Díaz, A., 2014, Modelo paleoambiental de la Formación Las Arcas (Mioceno Superior), quebrada del Mal Paso, Valles Calchaquíes del sur de Salta: Reunión Argentina de Sedimentología: 114. Puerto Madryn, Chubut, Abstracts, 2 p.
30. González, O.E., 1999, Geología de La Angostura, valle de Tafí, Tucumán: XIV Congreso Geológico Argentino, Abstracts, Actas I: p. 283–286.
31. González, O.E., 1990, Las vulcanitas del Portezuelo Las Ánimas, sierra de Aconquija, provincias de Catamarca y Tucumán: Revista de la Asociación Geológica Argentina XLV(3-4): p. 386–396.
32. Grier, M.E., Salfity, J.A., and Allmendinger, R.W., 1991, Andean reactivation of the Cretaceous Salta rift, NW Argentine: J S Am Herat Sci 4: p. 351–372.
33. Gutiérrez, A.A., 2000, Morphotectonic Evidences of the Sinestral Rotation of the Pampeanas Mountain Ranges, Argentina: Revista Profil, Band 18, XVII Simposio Latinoamericano de Geología, Stuttgart, Abstracts, 6 p.
34. Gutiérrez, A.A., Alderete, M.C., and Bortolotti, P., 1997, Geomorfología tectónica (neotectónica) en la sierra de La Candelaria, provincia de Salta: IV Simposio Argentino de teledetección, Resúmenes, San Juan, Abstracts, 9 p.
35. Gutiérrez, A.A., and Mon, R., 2008, Macroindicadores cinemáticos en el Bloque Ambato, provincias de Tucumán y Catamarca: Revista de la Asociación Geológica Argentina 63(1): p. 24–28.
36. Gutiérrez, A.A., and Mon, R., 2004, Megageomorfología del valle de Tafí-Aconquija, Tucumán: Revista de la Asociación Geológica Argentina 59(2): p. 303–311.
37. Gutiérrez, A.A., Mon, R., Arnous, A., and Aranda-Viana, R.G., 2021, Piedmont deposits as seismic energy dissipators, Sierras Pampeanas of Argentina: SN Applied Sciences (2021) 3:887, https://doi.org/10.1007/s42452-021-04874-0.
38. Gutiérrez, A.A., Mon, R., Arnous, A., and Cisterna, C.E., 2019, Sinestral rotation and NNW shortening of the ambato block induced by cenozoic NE to E-W transpression, Argentina: Int J Earth Sci Geol 1(2): p. 74–85. https://doi.org/10.18689/ijeg-1000109.
39. Gutiérrez, A.A., Mon, R., Cisterna, C.E., Altenberger, U., and Arnous, A., 2023, Cenozoic Age Counter clockwise Rotation in the Northwest End of the Sierras Pampeanas, Argentina: Open Journal of Geology, 13: p. 345–383. https://doi.org/10.4236/ojg.2023.135018.
40. Gutiérrez, A.A., Mon, R., Sàbat, F., and Iaffa, D.N., 2017, Origin and evolution of the salinas grandes and Salina de Ambargasta, Argentina: In: World multidisciplinary earth sciences symposium, IOP conference series: earth and environmental science, v.(95): p. 022–036. https://doi.org/10.1088/1755-1315/95/2/022036.
41. Gutiérrez, A.A., Mon, R., and Vergara, G., 2003, Neotectónica: captura y decapitación del drenaje, Tucumán-Argentina: Congreso Argentino de Cuaternario y Geomorfología, Abstracts, Tucumán, Actas II, p. 293–300.
42. Hanks, T.C., and Kanamori, H., 1979, A moment magnitude scale: J Geophys Res 84, p. 2348–2350.
43. Iaffa, D.N., Sàbat, F., Bello, D., Ferrer, O., Mon, R., and Gutiérrez, A.A., 2011, Tectonic inversion in a segmented foreland basin from extensional to piggyback settings: the Tucumán basin in NW Argentina: Journal of South American Earth Sciences 31: p. 457– 474.
44. Iaffa, D.N, Sàbat, F., Muñoz, J.A,, Mon, R., and Gutierrez, A.A., 2011, The role of inherited structures in a foreland basin evolution. The Metán Basin in NW Argentina: Journal of Structural Geology, 33: p. 1816–1828.
45. Ikeda, Y., 1983, Thrust front migration and its mechanisms-evolution of intraplate thrust fault

© 2023 Global Journals

systems: Bulletin of the Geography Department. Univ Tokyo 15: p. 125–159.
46. Incorporated Research Institutions for Seismology (IRIS), 2020, 1200 New York Av. NW Suite 400, Washington, DC 20005, 202- 682-2220. http://ds.iris.edu (accessed June 2023).
47. Instituto Nacional de Prevención Sísmica (INPRES), 2018, Reglamento INPRES-CIRSOC 103, Reglamento Argentino para construcciones sismorresistentes, Parte I: Ministerio dellnterior, Obras Públicas y Vivienda, Secretaría de Planificación Territorial y Coordinación de Obra Pública. 86 p.
48. Jakulica, D., 1948, Estudio geológico en la zona del cerro Colorado: YPF (informe inédito), Buenos Aires, DGE, 341, 18 p.
49. Jordan, T., and Alonso, R., 1987, Cenozoic stratigraphy and basin tectonics of the Andes Mountains, 20-28 South latitude: AAPG Bulletin 71(1): p. 49–64. https://doi.org/10.1306/94886D44-1704-11D7-8645000102C1865D.
50. Kamb, B., Silver, L.T., Abrams, M.J., Carter, B.A., Jordan, T.H., and Minster, J.B., 1971, Pattern of faulting and nature of fault movement in the San Fernando earthquake, in The San Fernando, California, Earthquake of February 9, 1971: U S Geol Surv Prof Pap 733: p.41–54.
51. Lavenu, A., 2006, Neotectónica de los Andes entre 1° N y 47° S (Ecuador, Bolivia y Chile): una revision: Revista de la Asociación Geológica, Argentina 61(4): p. 504–524.
52. Löbens, S., Sobel, E.R., Bense, F.A., Wemmer, K., Dunkl, I., and Siegesmund, S., 2013, Refined exhumation history of the northern Sierras Pampeanas, Argentina: Tectonics 32: p. 453– 472. https://doi.org/10.1002/tect.20038.
53. López, J.P., Altenberger, U., Bellos, L.I., Ferrocchio, B., and Llomparte Frentzel, G., 2017, Petrological and geochemical characteristics of El Pabellón granite, Tafí del Valle, Tucumán, NW of Argentina: XX Congreso Geológico Argentino, Sesión Técnica 4, Petrología y Geoquímica de Rocas Ígneas, Abstracts, San Miguel de Tucumán, Argentina, p. 62–68.
54. Marrett, R.A., Allmendinger, R.W., Alonso, R.N., and Drake, R.E., 1994, Late Cenozoic tectonic evolution of the Puna Plateau and adjacent foreland, Northwestern Argentine Andes: Journal of South American Earth Sciences 7(2): p. 179–207. https://doi.org/10.1016/0895-9811(94)90007-8.
55. Marshall, L.G., and Patterson, B., 1981, Geology and geochronology of the mammal-bearing Tertiary of the Santa María Valley and Corral Quemado River, Catamarca province, Argentina: Field Mus Nat Hist 9: p. 1–78.
56. McFarland, P.K., and Bennett, R.A., 2017, How do regional stress changes following megathrust events affect active retro arc tectonics? A case study of the 27 February 2010 Mw 6.1 Salta earthquake: AGU Fall Meeting Abstracts, G43A-0905, New Orleans, Louisiana, 2 p.
57. Mon, R., 1993, Influencia de la Orogénesis Oclóyica (Ordovícico - Silúrico) en la segmentación andina en el norte argentino: Decimosegundo Congreso Geológico Argentino, Abstracts, 3: p. 65–71.
58. Mon, R., and Drozdzewski, G., 1999, Cinturones doblevergentes en los Andes del norte argentino - Hipótesis sobre su origen: Rev. de la Asociación Geol. Argentina 54: p. 3–8.
59. Mon, R., and Gutiérrez, A.A., 2007, Estructura del extremo sur del Sistema Subandino (provincias de Salta, Santiago del Estero y Tucumán): Revista de la Asociación Geológica Argentina 62(1): 7 p.
60. Mon, R., Gutiérrez, A.A., Sábat, F., and Iaffa, D., 2012, A Miocene Continental Basin associated with the back thrusting of the Eastern Sierras Pampeanas in the Santa Maria Valley, Northwestern Argentina: Italian J Geosci (Boll.Soc.Geol.It.) 131(1): p. 123–135. https://doi.org/10.3301/IJG.2011.27 (Roma).
61. Mon, R., Gutiérrez, A.A., Vergani, G., Pacheco, M.M., and Sábat, F., 2005, Estructura de la depresión tectónica de Metán (Provincia de Salta): Actas del XVI Congreso Geológico Argentino, La Plata, Abstracts, p. 73–80.
62. Nortje, G.S., Olive, N.H.S., Blenkinsop, T.G., Keys, D.L., and Mclellan, J.G., 2011, Oxenburgh S (2011) New faults v fault reactivation: implications for fault cohesion, fluid flow, and copper mineralisation, Mount Gordon Fault Zone, Mount Isa District, Australia: In: Fagereng A, Toy VG, Rowland JV (eds) Geology or the earthquake source: a volume in honour of Rick Sibson. Geological Society, vol 359. Special Publications, London, p. 287–311.
63. Ortíz, P.E., and Jayat, J.P., 2007, Sigmodontinos (Rodentia: Cricetidae) del límite Pleistoceno - Holoceno en el valle de Tafí (Tucumán, Argentina): taxonomía, tafonomía y significación Paleoambiental: Ameghiniana, Revista de la Asociación Paleontológica Argentina, Buenos Aires, 44(4): p. 641–660.
64. Pearson, D.M., Kapp, P., De Celles, P.G., Reiners, P.W., Gehrels, G.E., Ducea, M.N., and Pullen, A., 2013, Influence of pre-Andean crustal structure on Cenozoic thrust belt kinematics and shortening magnitude: northwestern Argentina: Geosphere 9 (6): p. 1766–1782. https://doi.org/10.1130/ges00923.1.
65. Peña-Monné, J.L., and Sampietro-Vattuone, M.M., 2018, Paleoambientes holocenos del valle de Tafí (Noroeste Argentino) a partir de registros morfosedimentarios y geoarqueológicos: In: Polanco JM, Frugone M (eds) Boletín Geológico y Minero. Paleoclimas en Iberoamérica. Un análisis

© 2023 Global Journals

mediante registros geológicos e indicadores ambientales, vol 129(4): p. 671–691.
66. Peri, V.G., 2012, Caracterización morfotectónica de las Lomadas de Otumpa (gran Chaco, Santiago del Estero y Chaco): Influencias en el control del drenaje: Universidad de Buenos Aires, Facultad de Ciencias Exactas y Naturales, Departamento de Ciencias Geológicas [Tesis doctoral], 321 p.
67. Peri, V.G., and Rossello, E.A., 2010, Anomalías morfoestructurales el drenaje del río Salado sobre las Lomadas de Otumpa (Santiago del Estero y Chaco) detectadas por procesamiento digital: Revista de la Asociación Geológica Argentina 66(4): p. 634–645.
68. Pezzi, E.E., and Mozetic, M.E., 1989, Cuencas sedimentarias de la region Chacoparanaense. Cuencas sedimentarias Argentinas: Serie correlación geológica N° 6, Instituto Superior de Correlación Geológica, Universidad Nacional de Tucumán, p. 65–78.
69. Pilger, R., 1984, Cenozoic plate kinematics, subduction and magmatism South American Andes: J Geol Soc Lond 41: p. 793–802.
70. Pomposiello, C., Peri, V.G., and Favetto, A., 2010, Magnetotelluric model across the Chacopampeana Plain at 27° S, Santiago del Estero and Chaco provinces, Argentina: IAGA WG 1.2 on Electromagnetic Induction in the Earth 20th Workshop Abstract, Giza, Egypt, 4 p.
71. Porto, J.C., Danieli, C., and Ruiz-Huidobro, O.J., 1982, El Grupo Salta en la Provincia de Tucumán: V Congreso Latinoamericano Argentino, Abstracts, Actas IV: p 253–264.
72. Powell, J.E., and González, O.E., 1997, Hallazgo de mamíferos en la Formación Saladillo (Grupo Santa María), próximo al río Amaicha, provincia de Tucumán: Implicancias cronológicas. Ameghiniana 34: p. 124–130.
73. Ramos, V.A., Alonso, R.N., and Strecker, M.R., 2006, Estructura y neotectónica de Las Lomas de Olmedo, zona de transición entre los sistemas Subandino y de Santa Bárbara, Provincia de Salta: Revista de la Asociación Geológica Argentina 61(4): p. 579–588.
74. Ricci, H., and Villanueva, A., 1969, La presencia del Paleozoico inferior en la sierra de La Candelaria (provincia de Salta): Acta Geológica Lilloana, Tucumán, 10(1): p. 1–6.
75. Riller, U., and Oncken, O., 2003, Growth of the Central Andes Plateau by tectonic segmentation is controlled by the gradient in crustal shortening: Journal of Geology 111: p. 367–384.
76. Rodgers, D., and Rizer, W.D., 1981, Deformation and secondary fault- ing near the leading edge of a thrust fault: In Thrust and Nappe: Tectonics, Geol. Soc. London, Spec. Pub., (9): p. 65–77.
77. Rossello, E.A., and Veroslavsky, G., 2012, Definición del límite occidental del Sistema Acuífero Guaraní (Gran Chaco, Argentina): ¿técnico o convencional?: Boletín Geológico y Minero, ISSN: 0366-0176, 123(3): p. 297–310.
78. Ruiz-Huidobro, O.J., 1972, Descripción geológica de la Hoja 11 e, Santa María, provincias de Catamarca y Tucumán: Servicio Nacional Minero Geológico, Boletín, 134, 65 p.
79. Sampietro-Vattuone, M.M., and Peña-Monné, J.L., 2016, Geomorphological dynamic changes during the Holocene through ephemeral stream analyses from Northwest Argentina: CATENA 147: p. 663–677. https://doi.org/10.1016/j.catena.2016.08.029.
80. Sampietro-Vattuone, M.M., Peña-Monné, J.L., Roldán, J., Dip, A.B., Maldonado, M.G., Lefebvre, M.G., and Vattuone, M.A., 2019, Land management and soil degradation evidence during the Late Holocene in Northwest Argentina (La Costa 2 - Tafí Valley): Catena 182, Elsevier, 13 p.
81. Schellenberger, A., Heller, F., and Veit, H., 2002, Magnetostratigraphy and magnetic susceptibility of the Las Carreras loess-paleosol sequence in Valle de Tafí, Tucumán, NW de Argentina: paleoclimatic significance: XV Congreso Geológico, Calafate, Abstracts, Actas CD- ROM, Artículo N° 317, 4 p.
82. Scholz, C.H., 2002, Mechanics of earthquakes and faulting: 2nd ed. Cambridge University Press, New York. https://doi.org/10.1017/CBO9780511818516.
83. Schwanghart, W., and Scherler, D., 2014, TopoToolbox 2 e MATLAB - based software for topographic analysis and modelling in Earth surface sciences: Short Commun Earth Surf Sci Earth Surf Dyn 2(1): p. 1–7.
84. Sibson, R.H., 1982, Fault zone models, heat flow, and the depth distribution of earthquakes in the continental crust of the United States: Bull Seismol Soc Am 72: p. 151–163.
85. Somoza, R., and Ghidella, M.E., 2005, Convergencia en el margen occidental de América del Sur durante el Cenozoico: 16° Congreso Geológico Argentino, La Plata, Abstracts, Actas, p. 43–45.
86. Spagnuolo, C.M., Georgieff, S.M., and Rapalini, A.E., 2015, Magnetostratigraphy of the Miocene las Arcas formation, Santa María valley, northwestern Argentina: Journal of South American Earth Sciences 63: p. 101–113.
87. Starck, D., and Vergani, G., 1996, Desarrollo tecto-sedimentario del Cenozoico en el sur de la Provincia de Salta-Argentina: 13° Congreso Geológico Argentino, Buenos Aires, Abstracts, Actas 8: p. 433–452.
88. Strecker, M.R., Bloom, A., Carrión, M., Villanueva, A., and Naeser, C., 1984, Piedmont terraces in the Valle de Santa María and in front of southwestern

© 2023 Global Journals

Sierra Aconquija: Actas del 9° Congreso Geológico Argentino San Carlos de Bariloche, Abstracts, 2: p. 448–465.
89. Strecker, M.R., Bloom, A.L., Malizzia, D., Cerveny, P., Bossi, G.E., Bensel, C.H., and Villanueva-García, A., 1987, Nuevos datos Neotectónicos sobre las Sierras Pampeanas Septentrionales (26°-27° S), República Argentina: Décimo Congreso Geológico Argentino, San Miguel de Tucumán, Abstracts, 1: p. 231–234.
90. Strecker, M.R., Cerveny, P., Bloom, A.L., and Malizia, D., 1989, Late Cenozoic tectonism and landscape development in the foreland of the Andes: Northern Sierras Pampeanas (26°-28° S), Argentina: Tectonics 8: p. 517–534.
91. Turner, J.C.M., 1960, Estratigrafía de la sierra de Santa Victoria y adyacencias: Bol. Academia Nacional de Ciencias, Córdoba, 41(2): p. 163–196.
92. Wells, D.L., and Coppersmith, K.J., 1994, New empirical relationships among magnitude, rupture length, rupture width, rupture area, and surface displacement: Bull Seismol Soc Am 84: p. 974–1002.
93. Woodcock, N.H., and Fisher, M., 1986, Strike-slip duplexes: J Struct Geol 8(7): p. 725–735.
94. Zampieri, D., Gutiérrez, A.A., Massironi, M., and Mon, R., 2012, Reconciling opposite strike-slip kinematics in the Sierra Pampeanas (Argentina) transpressional belt: European Geosciences Union General Assembly, Viena, Austria, Abstracts, 2 p.
95. Zeckra, M., 2020, Seismological and Seismotectonic Analysis of the Northwestern Argentine Central Andean Foreland [Ph.D. thesis]: https://doi.org/10.25932/publishup-47324, Potsdam University, 118 p.

© 2023 Global Journals